1964

Microscopic observations on etched surfaces of zinc single crystals and on anodic disintegration.

Yun Wang

MICROSCOPIC OBSERVATIONS ON ETCHED SURFACES OF ZINC SINGLE CRYSTALS AND ON ANODIC DISINTEGRATION

BY

YUN WANG, 1919-

A

THESIS

submitted to the faculty of the

SCHOOL OF MINES AND METALLURGY OF THE UNIVERSITY OF MISSOURI

in partial fulfillment of the work required for the

Degree of

MASTER OF SCIENCE IN METALLURGICAL ENGINEERING

Rolla, Missouri

1964

Approved by

M. E. Straumanis (Advisor) W. J. James

A. P. Leighly Jr. Paul Dean Proctor

ABSTRACT

The technique used to grow single zinc crystals was based on the Bridgman method. Zinc-gold, zinc-aluminum, and zinc-magnesium alloys were prepared and their single crystals were grown. Four crystallographic planes of the single zinc crystals were used for both chemical and anodic etching. The zinc alloys were etched more easily by acids than the purest (99.999%) zinc. The etching patterns changed for the different crystallographic planes of the single zinc crystals.

The appearance of particles during anodic dissolution of the single zinc crystals depended on time, acid concentration and current density. The partial disintegration of single zinc crystals is promoted by strong and prolonged etching. Four acids (HCl, $HClO_4$, H_2SO_4 and HNO_3) were used as etchants; of them hydrochloric acid was the most effective. The particles were examined under high magnification with oil immersion. The black tiny particles with metallic luster were opaque to light, suggesting the presence of zinc metal.

The degree of disintegration of single zinc crystals in neutral salt solutions was determined quantitatively. The partial disintegration of a dissolving zinc anode in a 3 percent sodium bromate solution was studied. The apparent valence of Zn ions in bromate solution was smaller than that in nitrate solution. The degree of disintegration of zinc in bromate solution was about three times of that in nitrate

solutions. The crystal structure and orientation do not affect the partial disintegration of zinc in nitrate and in bromate solutions to a noticeable extent. The dark film formed at the beginning of electrolysis, was obtained after twenty seconds by dipping the zinc anode into dry acetone. The flakes which spalled from the anode were collected and examined optically. They were composed of many small metallic zinc particles embedded in a matrix of zinc hydroxide. After thirty seconds of electrolysis the dark film gradually turned white and fell into the electrolyte.

The conclusion is that the normal valence of zinc ion does not change during anodic dissolution in bromate solutions, but rather that the apparent valence of less than two arises as a consequence of partial disintegration of the anode. The dissolution of zinc outside the electrical circuit thus accounts for the lower coulombic equivalent.

ACKNOWLEDGMENTS

The author wishes to express his gratitude to Dr. M. E. Straumanis, Research Professor of Metallurgy, for his guidance and assistance in the pursuit of this research.

He is also indebted to the Missouri School of Mines and Metallurgy and to the Corrosion Research Council for financial support of this project.

Sincere thanks are due to the various members of the faculty for their help and suggestions throughout this investigation.

TABLE OF CONTENTS

Page

LIST OF FIGURES

Figures Page

Figures Page

Figures Page

LIST OF TABLES

I. INTRODUCTION

Zinc is a very active and important metal in the field of corrosion, although it is actually not known how the metal is attacked by acids, and how the corrosion process penetrates into the depth of a sample. The primary objectives of this research were to observe and to study this process of destruction and the formation of etch pits of the corroded surfaces of both pure and impure zinc. However, polycrystalline material is inadequate for such studies, because the direction of the attack of the single crystallites cannot be determined. Therefore, single crystals consisting of pure Zn and of some of its diluted alloys were used. For single crystals, each crystal plane has a definite crystallographic structure extending throughout the whole crystal. Complications due to grain boundaries and difficulties arising from change in orientation of neighboring grains are, therefore, eliminated. Consequently, growth of single crystals of pure zinc and of zinc base alloys was a prerequisite for this investigation.

For the preliminary study polycrystalline Zn was also used. However, a search for new phenomena during the attack of Zn by acids and during anodic disintegration was also initiated. This phenomenon is disintegration of metals. How does disintegration of Zn single crystals occur? What is the degree of disintegration? Does pure Zn disintegrate in the same manner as the impure metal? What are the causes of disintegration? Efforts will be made to give an answer to these questions.

II. REVIEW OF THE LITERATURE

A. Methods Used for Growing Single Metal Crystals.

The first good method for producing large metallic crystals was that of Bridgman which was published in 1925[1]. His method was that of slow solidification from the melt. An electric furnace in the vertical position was maintained at a temperature above the melting point of the metal in question. The metal in the molten condition in a mold of glass or quartz tubing was slowly lowered through the bottom of the furnace into the air of the room. Solidification thus started at the bottom of the tube and proceeded slowly along its axis, keeping pace with the lowering. If the lowering were at a speed less than the velocity of crystallization and also slow enough so that the latent heat of solidification was dissipated by conduction, then the metal usually crystallized as one grain, provided that only one nucleus started in the tube at the bottom.

In 1950, D. C. Jillson[2] published a description of a method and the equipment used for the growth of high purity single zinc crystals. He did not lower the tubing with the liquid metal through the furnace as Bridgman did, but lowered the temperature by slowly decreasing the power input. The tubing was held stationary in the furnace in one position.

In 1951, M. A. Steinberg[3] grew single crystals of zinc and of some other low melting point metals by using the Bridgman technique. The temperature gradient within the furnace and the rate of movement of the containers of molten metals through the furnace were controlled. The equipment

was shock mounted for the prevention of vibration. Using a special holder for specimens 1/4 inch in diameter, a dozen crystals could be grown simultaneously. Thus Jillson and Steinberg both used the Bridgman method with minor modifications.

B. Apparatus Designed for Cutting Single Metal Crystals.

To cut metal single crystals in certain crystallographic directions without straining and deforming them is another problem.

In 1950, Maddin and Asher[4] constructed an etch cutter which consisted of a goniometer, polystyrene drum, and two acid baths. The crystals were cut by a plastic thread, i.e., saran string which constantly was wetted by the acid from the 2 acid baths. The drum was driven by a 1 r. p. m. reversible motor.

In 1956, Yamamoto and Watanabe[5] constructed a similar but improved etch cutter based upon Maddin and Asher's design where the rotation of the drum was controlled at any desired speed. The experimental results regarding the different metal crystals, etching solutions, string material, and the conditions of cut surface were tabulated in the publication. It is a worthy reference in this field.

In 1959, Reitsma[6] constructed an etch cutter in this School for cutting indium crystals without recrystallization, the construction of which was copied, in its more important details, from the design of Yamamoto and Watanabe. Most of the cutter was made of polyethylene which is resistant to

acid attack. Reitsma, in copying Yamamoto's etch cutter made it simpler and more economical.

C. Chemical and Anodic Etching of Metals.

After cutting and polishing a specimen the third step is etching. The purpose of etching is to clean the surface, remove the damaged surface layer, revealing etch pits and the structure of the section through the crystals.

The etchants can be grouped into two categories:

1. Preferential etchants produce pits whose facets have a definite crystallographic orientation. Bassi and Hugo in 1959[7] produced etch pits on zinc by chemical etching after electrolytic polishing. Another study was made by Bicelli and Rivolta in 1961.[8] They investigated the planes (0001) and (1120) of zinc single crystals attacked by various acids and other solutions. The geometrical figures (hexagons) were usually obtained on the (0001) surface but they seldom occurred on the (1120) plane.

2. Nonpreferential etchants not only produce a polished surface but also reveal dislocations. Gilman[9] described a technique for producing etch pits at the site of edge dislocations of zinc monocrystals in 1956, and George[10] observed star-shaped terraced etch pits at the sites of dislocations of zinc crystals in 1959.

The etchants used for this research were both preferential and nonpreferential.

D. Disintegration Phenomena of Metals.

The metallic particles are detached from the metal itself.

When a metallic specimen dissolves anodically in a corrosive liquid, the weight loss is greater than calculated from Faraday's law. According to Evans "anodic corrosion eats its way along grain-boundaries, so that the grains themselves drop out unchanged, causing a weight-loss greater than the calculated value".[11] The same phenomenon was also observed by some other investigators. Free Mg particles were observed by Hoey and Cohen in 1958.[12] "Disintegration" of electrodes was proposed by Marsh and Schaschl in 1960[13] for the explanation of the negative difference effect and for corrosion of steel in aqueous solutions. However, all the particles observed were large chunks, which occasionally dropped out during dissolution as described by Evans. In recent years it has been noted in this laboratory that metals also disintegrate during dissolution into very fine particles, not observed by other investigators. Articles were published regarding partial disintegration of Be in $HClO_4$[14] and in HCl[15] and that of Mg in $HClO_4$[16]. As for the disintegration of Zn in nitrate solutions, a note was written by James and Stoner in 1963.[17]

Summing up, the author believes that the most important papers regarding growing, cutting, and etching of single Zn crystals have been reviewed as the four sections of this paragraph. There are no publications concerning disintegration of single Zn crystals.

III. EXPERIMENTAL

The experimental plan consisted of the following three major phases:

A. The preparation of single zinc crystals, B. the observations made on crystals of zinc and its alloys etched by acids, C. the study of anodic disintegration of zinc crystals in bromate solutions.

The description of each phase includes apparatus, procedures, and experimental results.

Materials

The materials used were zinc, chemical reagents and the alloying elements.

1. The zinc used for the growth of single crystals was from two sources:

a. Pure zinc sticks (99.99%) were purchased from Fisher Scientific Company. Their composition was as follows:

As	0.000001%
Fe	0.002%
Pb	0.005%
Zn	balance.

b. High-purity zinc rods (99.99+%) were purchased from the American Smelting & Refining Company. Spectrographic analysis as furnished by them listed the following impurities:

Mg	<0.0001%
Pb	0.002%

Si.....<0.0001%

Fe.....0.0001%

Cu.....0.001%

Ag.....0.0005%

Sb, Tl, Mn, Sn, Cr, Ni, Bi, Al, Ca, In, and Cd were not detected by Standard Spectrographic Methods.

c. Zinc spatters of still higher purity (99.999+%) were also purchased from the American Smelting & Refining Company, and the impurities found spectrographically were the following:

Mg.....0.0001%

* Pb.....0.0001%

Si.....0.0001%

* Cu.....0.0003%

Cd.....0.0001%

Ag.....0.0002%

Sb, Tl, Mn, Sn, Cr, Fe, Ni, Bi, Al, Ca, and In were not detected by Standard Spectrographic Methods.

(* Chemical Analysis)

2. The chemicals (HCl, H_2SO_4, $HClO_4$, HNO_3, KNO_3, $NaBrO_3$, etc.) were of reagent grade.

3. The alloying elements used were gold (99.999%), aluminum (99.999%), and magnesium (99.995%).

A. <u>The Preparation of Single Zinc Crystals.</u>

All single zinc crystals were grown using the Bridgman method. The apparatus, procedure, and results are as follows:

1. <u>Apparatus.</u> For obtaining single crystals, a tube

furnace was constructed. The core of the furnace was 9 millimeters in diameter and 23 centimeters long. The Ni-Chrome wire was wound on the external surface of the core which was insulated with high temperature alundum cement. For prevention of the circulation of cold air through the core, a glass jar was put against the bottom of the furnace. The body of the furnace was made of six insulation bricks and whole was covered with aluminum sheets. The line voltage of the power source was 120 volts and about five amperes of the current was allowed to pass through the wire.

A clock mechanism was used for lowering the sample through the furnace. To change the speed of lowering a brass drum was lathed into five different sections, each of a different diameter, and connected with the driving mechanism. The test run of the clock motor indicated that one revolution was accomplished in 14.5 minutes. The required radii for each section of the drum were so calculated that a linear speed of the spinning line of 1 cm/hr, 1.5 cm/hr, 2 cm/hr, 4 cm/hr, and 5 cm/hr was reached. The complete apparatus consisted of the furnace, the driving mechanism, the temperature regulator, the powerstat, a stand, and a pulley with the spinning line. (see Fig. 1 and 2)

2. Procedure. According to the experimental plan, it was necessary to have single crystals of pure zinc and of zinc alloys. Based upon the potential series of metals, gold is more noble than zinc, but aluminum and magnesium are less noble than zinc, so gold, aluminum and magnesium

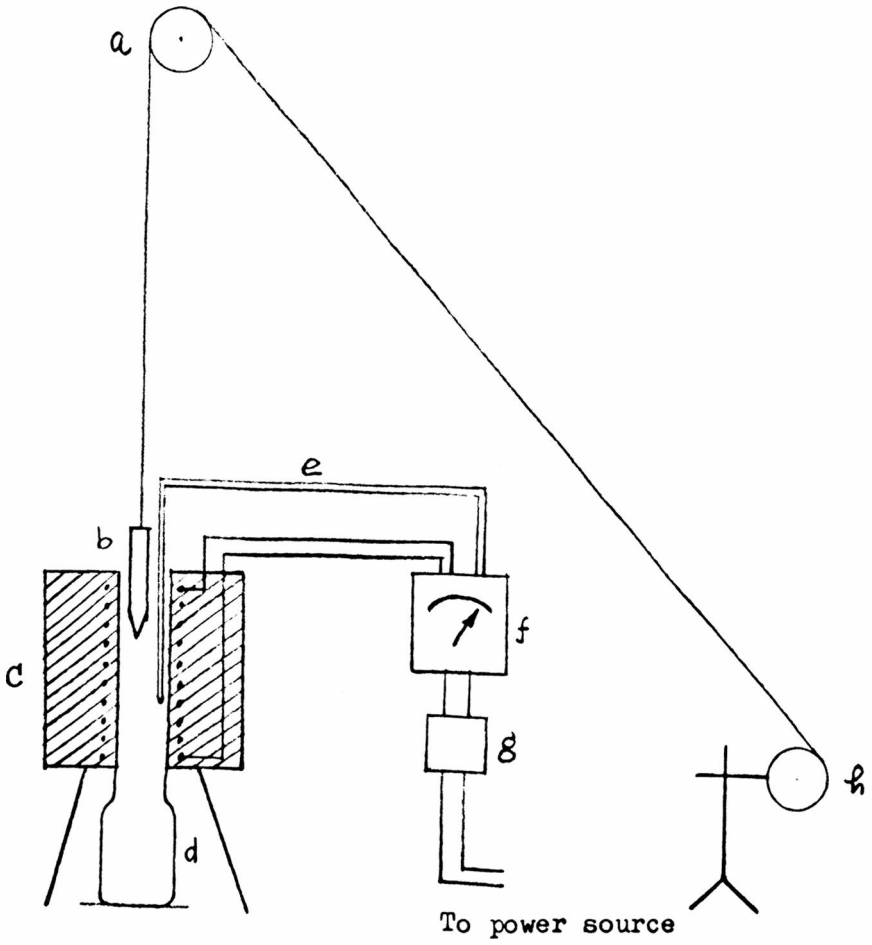

Figure 1.

Arrangement of apparatuses for growing single crystals.

a) Pulley.

b) Pyrex glass tube containing zinc specimen.

c) Tube furnace.

d) Glass jar.

e) Thermocouple.

f) Temperature regulator.

g) Powerstat.

h) Driving mechanism.

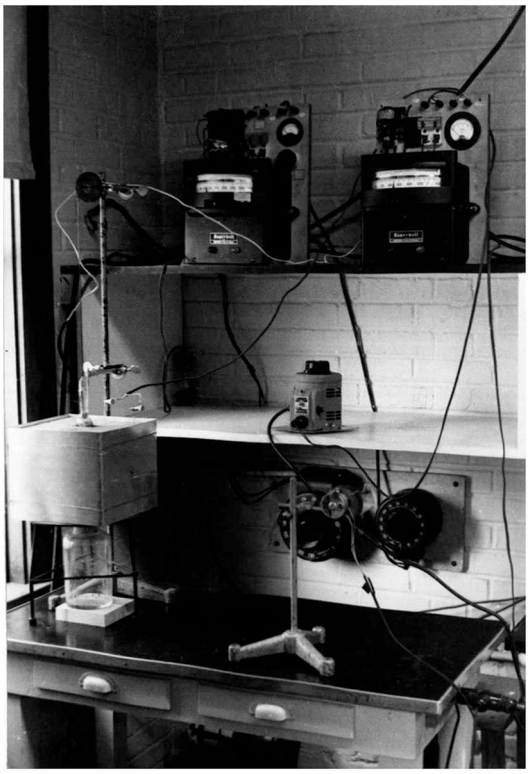

Figure 2.

Apparatus for growing zinc single crystals.

were chosen to alloy with pure zinc respectively, to see how these alloying elements affect the properties of zinc during etching by acids and anodic dissolution in neutral salt solutions.

First, pure gold splatters were intentionally added to the pure zinc metal in an attempt to see how gold affects the etching pattern of purest Zn. According to Westgren and Phragmen,[18] the solubility of Au in solid Zn at room temperature is about 5% by weight. The a parameter of the hexagonal Zn lattice is increased and c is lowered upon addition of Au.

For the preparation of a 1% master alloy, the proper amounts of gold and zinc were weighed on an analytical balance to $\pm$0.0001 gram and placed in a pyrex glass tube, evacuated and sealed. It was heated at 500°C for 72 hours, and shaken twice a day to promote complete miscibility of the two elements. From the master alloy the three other Zn-Au alloys were prepared by heating them for 48 hours at 500°C, and shaking them twice a day. All the samples were furnace cooled. The alloys were sectioned by sawing in half, the sections polished, etched with 8N nitric acid and examined at low magnification for appearance of segregations and distribution of the gold in the solid solution. Single crystals were grown from the 3 Zn-Au alloys of a composition shown in Table I.

TABLE I

Composition of Zinc-Gold Alloys

Alloy No	Weight percent Gold (99.999%)	Weight percent Zinc (99.99+%)
Master alloy	1.00	99.00
Alloy No. 1	0.01	99.99
Alloy No. 2	0.02	99.98
Alloy No. 3	0.04	99.96

As aluminum is less noble than zinc, aluminum was chosen as an alloying element for making Zn-Al alloys. The solid solubility of Al in Zn is, according to Hansen,[19] approximately 0.05% by weight at room temperature. Several Zn-Al alloys (Table II) were prepared by the same procedures as were the Zn-Au alloys, except that the Zn-Al alloys were air ccoled after heating.

TABLE II

Composition of Zinc-Aluminum Alloys

Alloy No.	Weight percent Aluminum (99.999%)	Weight percent Zinc (99.99+%)
Master Alloy	2.00	98.00
Alloy No. 4	0.005	99.995
Alloy No. 5	0.025	99.975
Alloy No. 6	0.05	99.95

Zn-Mg alloys (Table III) were prepared in the same manner as Zn-Al alloys. The solid solibility of Mg in Zn was reported

to be less than 0.002% Mg by weight at room temperature by Anderson and Rodda[20].

TABLE III

Composition of Zinc-Magnesium Alloys

Alloy No.	Weight percent Magnesium (99.995%)	Weight percent Zinc (99.99+%)
Master Alloy	2.00	98.00
Alloy No. 7	0.005	99.995
Alloy No. 8	0.01	99.99
Alloy No. 9	0.025	99.975

The second step was to grow single Zn crystals. The pure zinc sticks, high-purity zinc rods, and special high-purity zinc splatters, were used separately for growing single crystals. A pyrex glass tube having a conic end was used to contain the zinc metal. The glass tube was evacuated and sealed. After the temperature of the furnace had reached 500°C, the glass tube was lowered through the furnace at a speed of one centimeter per hour. When the glass tube was completely lowered into the empty glass jar out of the furnace, the furnace and the driving mechanism were both shut off, and the sample was cooled in the glass jar.

A single Zn crystal showed six reflections in the light beam when the crystal was rotated 360 degrees around its axis because of its hexagonal symmetry. Under the microscope only one orientation of the crystal could be seen on the etched surface; this confirmed it to be a single crystal.

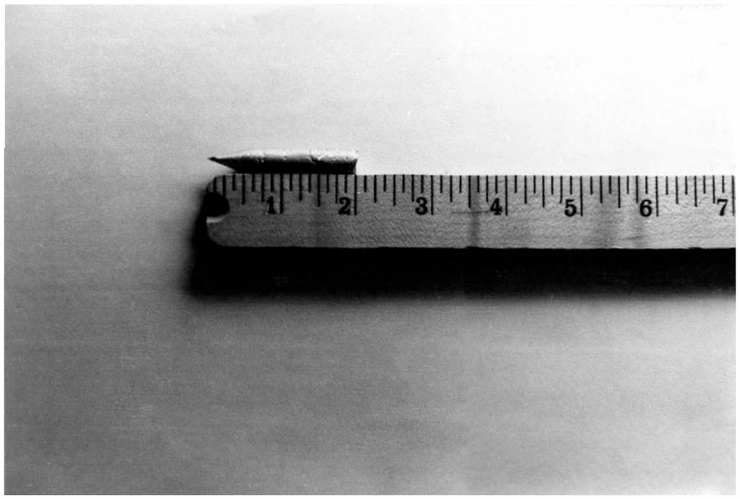

Figure 3.

Pure zinc single crystal, about 2 in. (5 cm) long.

The size was about 9 millimeters in diameter and 5-7 centimeters long (Fig. 3).

The time for growing one single crystal was about 20 hours. Caution must be taken when the sample is passing through the furnace and it should not be disturbed. For this reason the operation was done overnight. If the end of the pyrex glass tube were round instead of conic, several intergrown crystals instead of a single one were obtained. Single crystals of Zn-Au, Zn-Al, and Zn-Mg alloys were obtained in the same way. Some segregation was observed in Alloys No. 8 (0.01 wt. % Mg) and No. 9 (0.025 wt. % Mg).

After the furnace was built, about two dozen single Zn crystals were made.

The third step was to cleave and to cut the single crystals. The single Zn crystals were cleaved along their basal planes after they were cooled in liquid nitrogen. The cleavage could easily be achieved by putting the blade of a knife parallel to the basal plane of the single crystal. By gently hammering the blade, the crystal would split into two halves with the (0001) as a cleaving plane. The single crystals of zinc alloys were cleaved in the same manner.

Reconstruction of the etch cutter (Figs. 4 and 5) made by Reitsma in 1959 was done for the purpose of cutting single crystals in certain directions. The saran wire was used as sawing material which carried 8N HNO_3 as a cutting solution. Two plastic combs were fixed on the sides of the v-shaped specimen holder to prevent slipping of the saran wire during

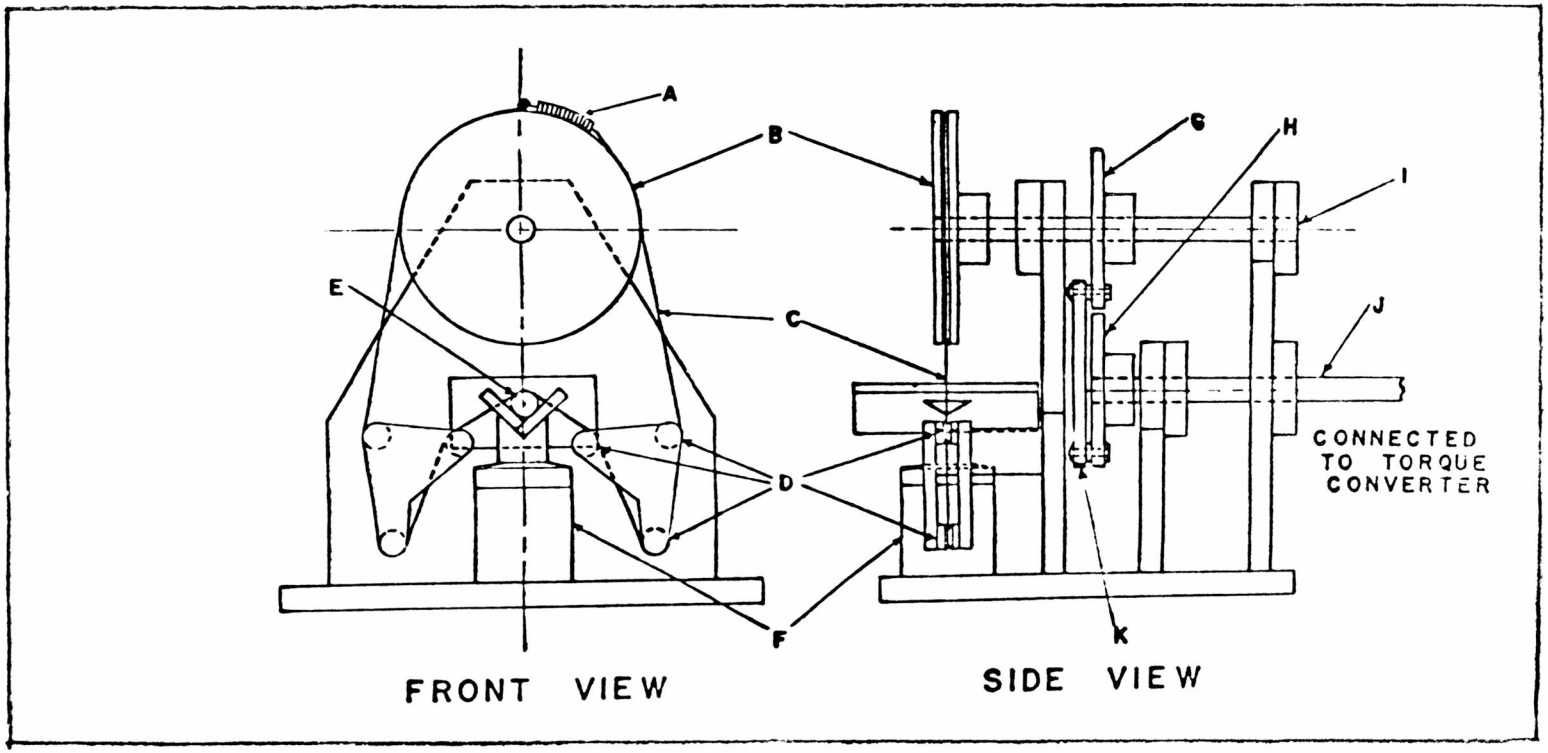

Scale 1/2" to 1"

Figure 4 Sketch of etch cutter

A Spring
B Drum
C Saran thread
D Rollers
E Specimen
F Goniometer & specimen holder
G Main drive wheel
H Auxiliary drive wheel
I Main shaft
J Auxiliary shaft
K Drive link

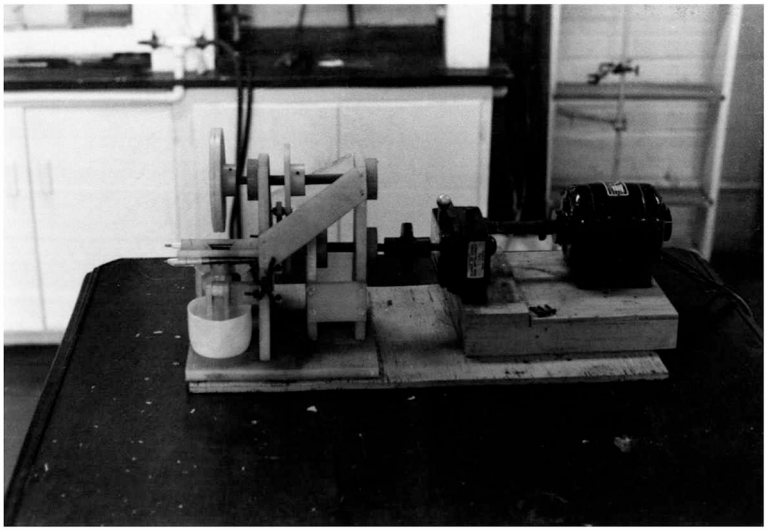

Figure 5.

Etch Cutter.

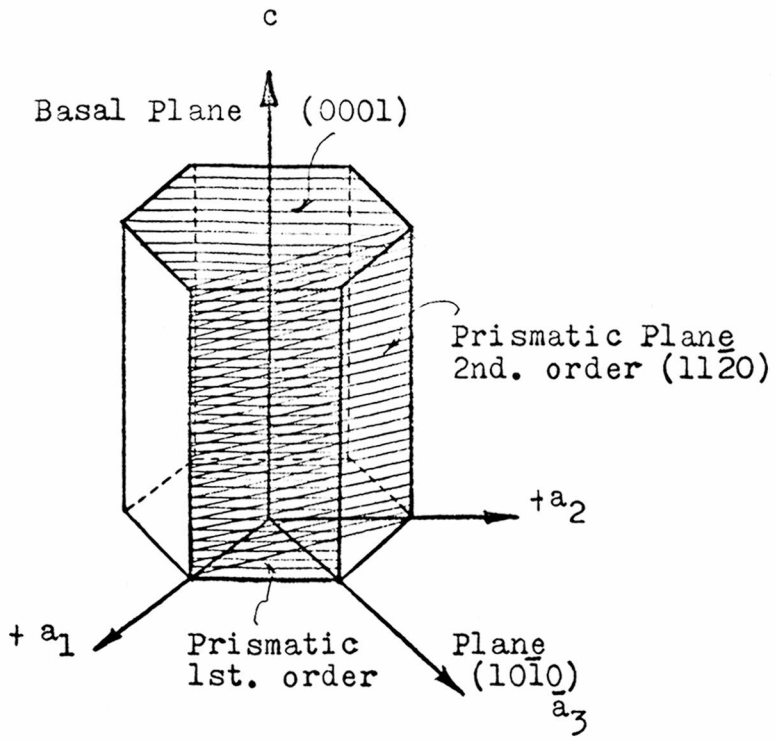

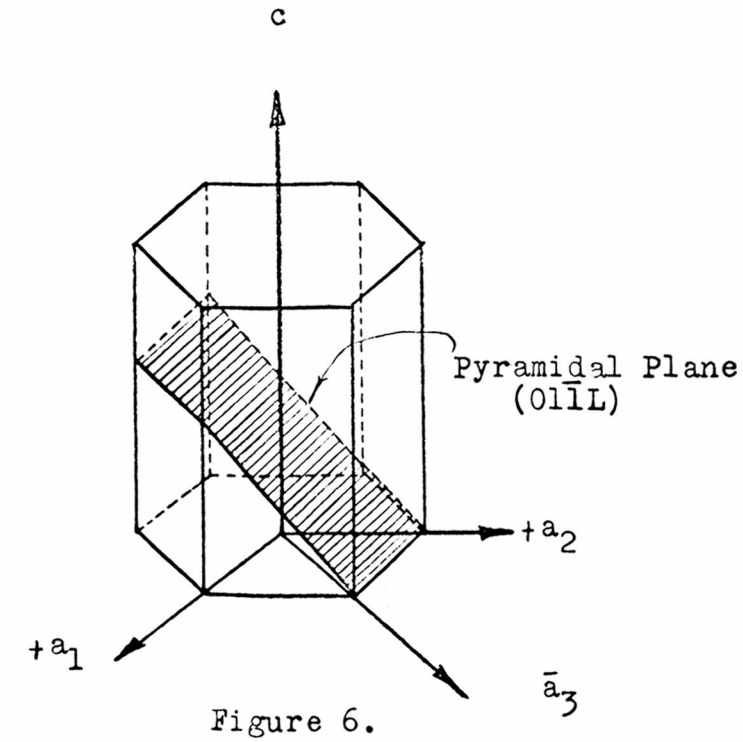

Figure 6.

Diagram of the cuts laid through a zinc single crystal.

operation. The time required for cutting a single crystal of 9 mm in diameter was about one hour. As the cut surface was slightly ragged, it was gently ground on 0, 2/0, 3/0, and 4/0 emery paper to smooth the surface. After grinding the deformed surface layer was removed by etching. Four crystallographic surfaces were used for the etching and disintegration observations: the (0001) - without cutting, the prismatic plane of first order $(10\bar{1}0)$, the prismatic plane of second order $(11\bar{2}0)$, and the pyramidal plane $(01\bar{1}L)$ respectively. The cuts as laid through the metal crystals are shown schematically on Fig. 6.

B. The Observations Made on Crystals of Zinc and its Alloys Etched by Acids.

For observing the formation of etch pits and the corrosion process, the purest Zn single crystals just described were employed. As for the specimens of high-purity zinc and its alloys, only two crystallographic planes were used for etching. The process of anodic etching was studied with pure Zn (99.99%) anodes. HCl was the main etchant, but H_2SO_4, $HClO_4$ and HNO_3 were also used.

1. Apparatus. An electrolytic system was set up for anodic treatment. (Fig. 7). After etching the specimens were observed under a Reichert Research Microscope.

2. Procedure. The chemical etching technique was performed by immersing clean specimens into the etching solution for a certain period of time, then the solution was quickly poured off and the specimens were washed and dried.

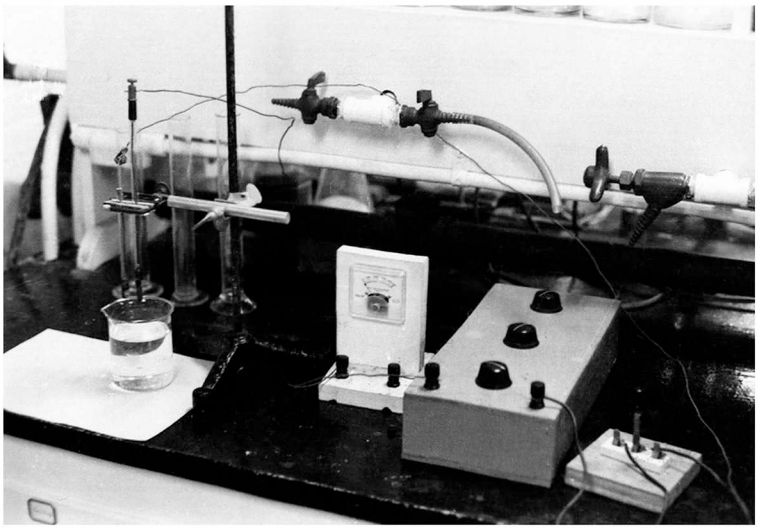

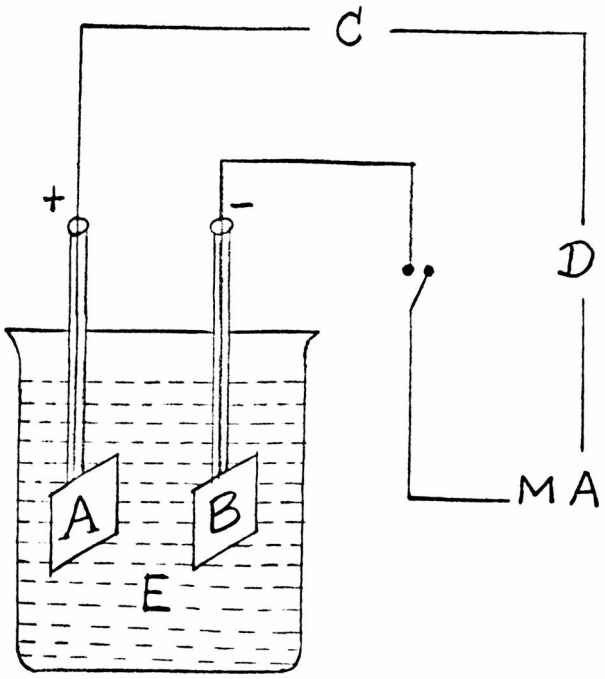

Figure 7. Electrolytic system.

A - Zinc anode

B - Platinized Pt cathode

C - Battery

D - Variable resistance

E - Electrolyte

Sometimes to remove oil placed on the specimen for high magnification observation, acetone had to be used to clean the surface before washing.

Prior to the anodic etching the surface of the specimen had to be very clean and smooth. The electrolytic circuit was closed before the specimen was immersed. By so doing the current could immediately pass through the circuit as soon as the specimen was in the electrolyte. To stop the etching, both electrodes were taken out of the electrolyte and then the circuit was opened. Usually the time applied for etching varied from a few seconds to several minutes. The concentration of the acid was changed from 2N, 6N, to 12N, and the current density was adjusted from a lower to a higher value.

3. Experimental results.

a. The basal plane. Before etching the basal plane of any crystal, the virgin surface of a specimen was studied through the interference tester of the microscope in monochromatic light obtained by a filter. When the specimen was brought into contact with the test plate, the microscope showed simultaneously the surface details of the specimen and the interference fringes. The interference fringes or rings were concentric circles around the point of contact. (Fig. 8). This indicated that the surface of the specimen was quite even without any irregularities on it.

After studying the unetched (0001) surface of the specimen the purest Zn single crystal with the (0001) surface was etched with 2N HCl for 20 sec. No etch pattern

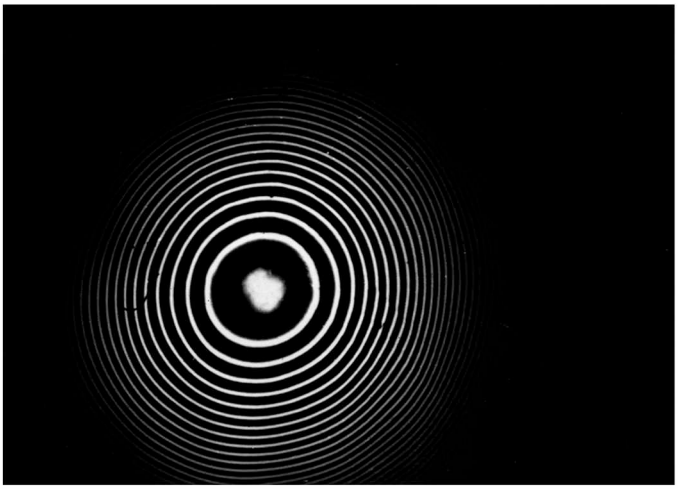

Figure 8.

Zn-Mg alloy, 0.005% Mg, single crystal, basal plane. Interference pattern of unetched cleavage surface. Magnification 165X.

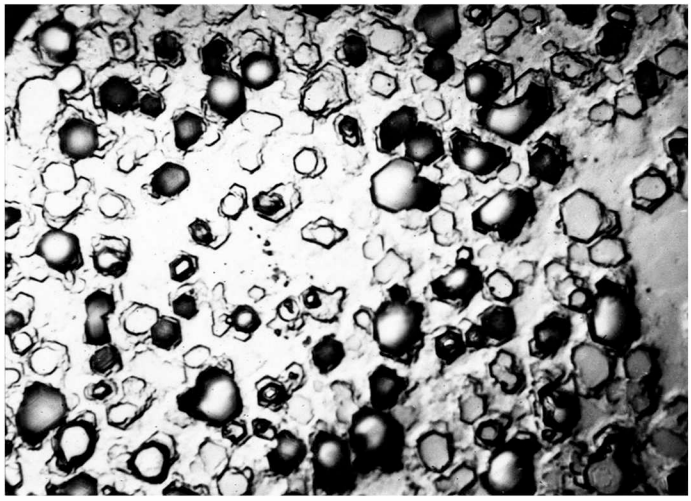

Figure 9.
Zn (99.999+%), single crystal, basal plane, etched in 2N HCl for 20 sec. Magnification 750X.

Figure 10.
Zn (99.99%), single crystal, basal plane, etched in 6N HCl for 10 sec. Magnification 1430X.

developed, so the etching was continued by touching the surface with a Pt needle to promote the process of corrosion. The crystal surface became slightly etched; the hexagons were visible only in the vicinity of the needle. Thus at some places there were numerous etch pits, while at other places, there were less. The depth of the etch pits was very shallow, and their size was small. (Fig. 9).

If the concentration of HCl was increased to 6N, a typical "leaves" etching pattern was obtained in only 10 sec. (Fig. 10). By prolonging the etching time to 80 sec., deeply etched surfaces were obtained. Fig. 11 (below) was taken when the camera was focused on the lower level (bottom) of the etch pits. The etching pattern appears clearly in the figure, because the bottom was very even. The dark portions, which were much higher (Fig. 11 top), looked like mountain peaks. The black portions with the highest points were scattered over the white portion as if they stuck to the surface of the specimen. A closer observation showed that the black points were particles which still adhered to the crystal surface. The identification and explanation of the nature of the surface disintegration of the dissolving crystal will follow. The top of Fig. 11, the white portion was out of focus, because the camera was focused on the upper level of the ridges. The difference between the ridges and the lower levels was about 7.5 microns. This result shows how the corrosion penetrated

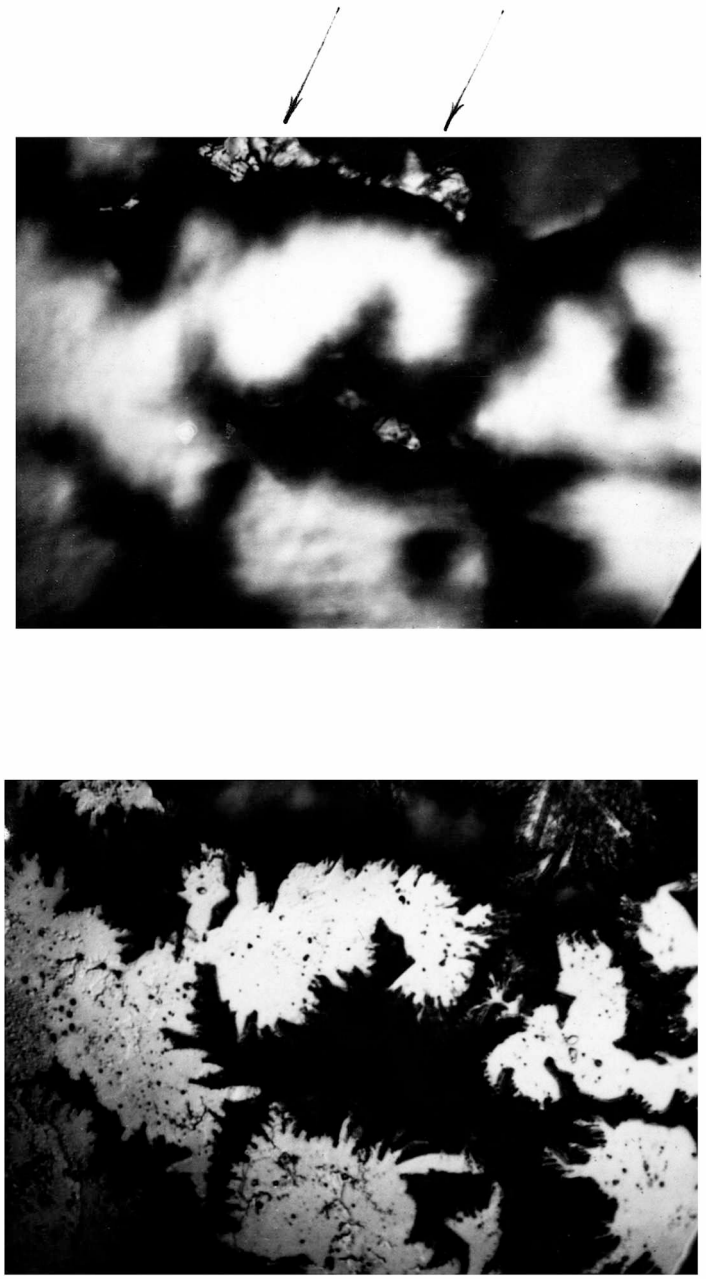

Figure 11.

Zn (99.99+%), single crystal, basal plane, etched in 6N HCl for 80 sec. Magnification 750X.
above - Upper level of etch pits.
below - Lower level of etch pits.

into the depth of the crystal starting from the (0001) plane.

HCl of a still higher concentration produced a "branched" etching pattern shown in Fig. 12. The white portions extended to larger areas and were lower than the dark branches. Black points were spread all over the surface. If the same crystal was etched with concentrated HCl (12N) for 10 sec., many hexagonal etch pits appeared. Some black (disintegrated) material collected in the centers of these hexagonal etch pits. Many big pits (Fig. 13) showed "steps" going down to the bottom of the pits. A pit with black (disintegrated) material in it can also be seen in Fig. 14. This specimen had a bright surface as if electropolished. The black points on the surface could be washed off with cotton. This figure showed several characteristics: (1) the geometrical shape of the etch pit was changed, (2) many "steps" were observed; dark material accumulated in the center of the bottom of the etch pit, (3) the pit was very deep. Another etching effect by concentrated HCl is shown in Fig. 15. The same specimen (of Fig. 14) was etched with the acid for 15 sec. The reaction proceeded violently; the specimen became smooth and shiny after etching and no salt was observed on the surface of the specimen. When it was washed with cotton, some black particles were washed away, but some particles were still sticking to the surface of the specimen. Nearly perfect hexagonal etching objects were observed; one of them is

Figure 12.
Zn (99.999+%), single crystal, basal plane, etched in 9N HCl for 15 sec. Magnification 750X.

Figure 13.
Zn (99.999+%), single crystal, basal plane, etched in 12N HCl for 10 sec. Magnification 750X.

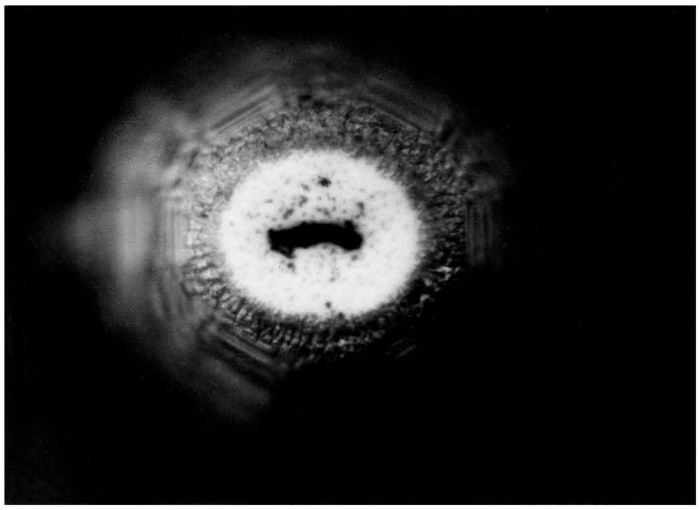

Figure 14.
Zn (99.99+%), single crystal, basal plane, etched in 9N HCl for 20 sec. Magnification 1430X.

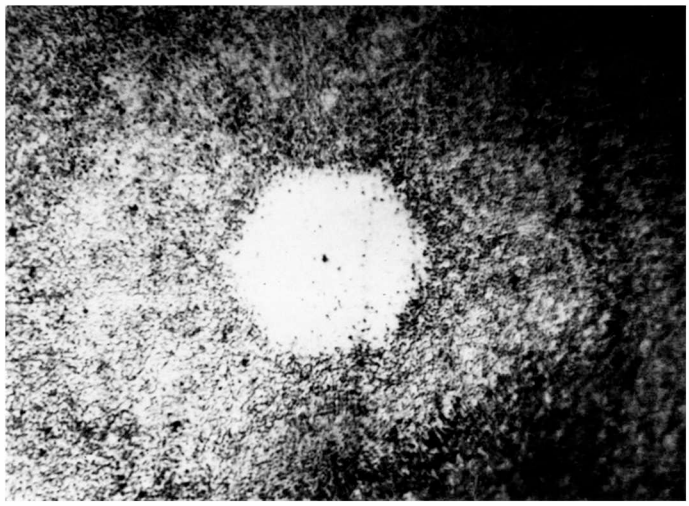

Figure 15.
Zn (99,99+%), single crystal, basal plane, etched in 12N HCl for 15 sec. Magnification 1430X.

shown in the center of Fig. 15. The photograph was taken after the specimen was washed. Under the microscope the etch pit appeared higher than its surroundings, as the area around the hexagon was attacked more vigorously than the hexagon area, which appeared to be a "negative" etch pit.

To find an answer to the nature of the black material in the etch pits and on the high elevations, a section through a high-purity zinc rod (99.99+%) was etched with 12N HCl for 20 sec. The dark material in and around the etch pits (Fig. 16) was removed from the surface of the specimen by a piece of Scotch tape. The tape was put on a thin piece of glass and observed under a microscope: black and shiny particles could be seen even at low magnification (Fig. 17). Nevertheless, as more particles had to be obtained for examinations, the specimen was etched in 12N HCl for 1 min. The particles obtained were transferred to the glass and examined under transmitted light at high magnification under the microscope with an oil immersion objective. The black metallic and shiny particles could be clearly recognized as shown in Fig. 18. The tiny particles with metallic luster were opaque, only the free parts of the Scotch tape were transparent to light. No salts were observed with this sample. The particles originated from the zinc crystal by disintegration of the surface layers due to strong etching.

The second kind of acid used to etch the (0001)

Figure 16.
Zn (99.99+%), polycrystalline, etched in 12N HCl for 20 sec. Magnification 575X.

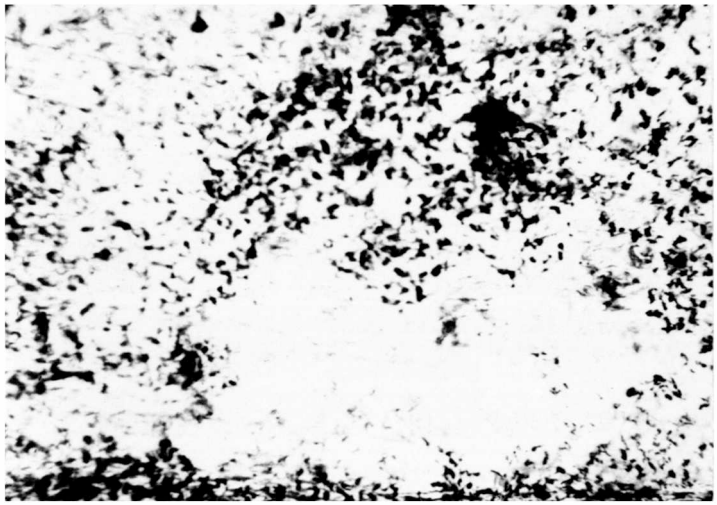

Figure 17.
Black particles removed from Zn (99.99+%) polycrystalline, etched in 12N HCl for 20 sec. Magnification 145X.

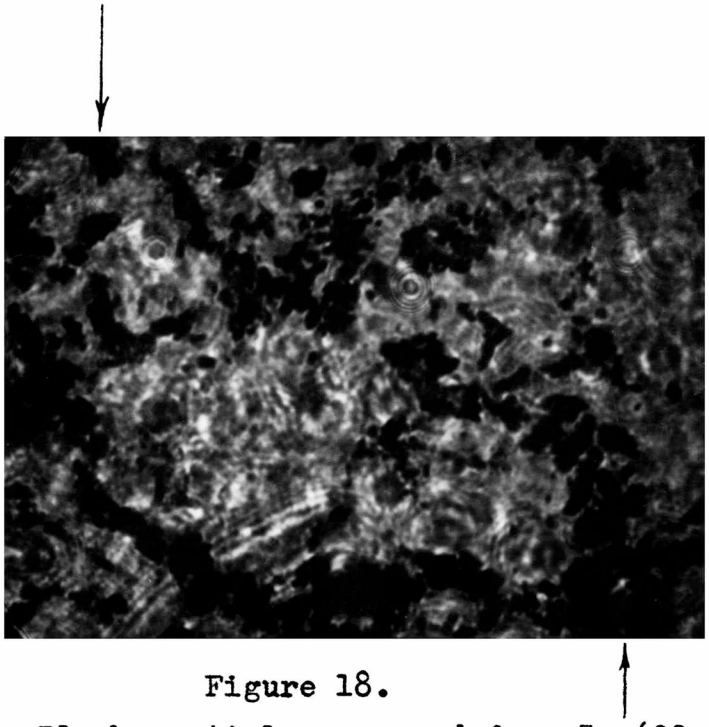

Figure 18.
Black particles removed from Zn (99.994%) etched in 12N HCl for 1 min.
Transmitted light. Magnification 1430X.

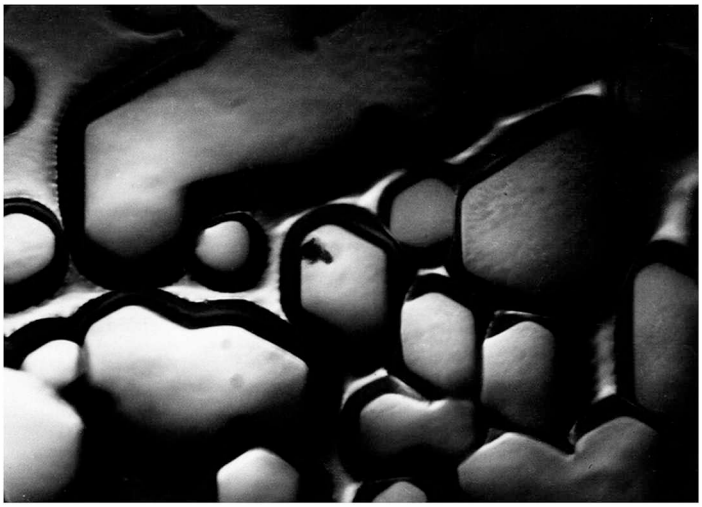

Figure 19.
Zn (99.99%), single crystal, basal plane, etched in 9.5N HNO_3 for 5 sec.
above - Top of etch pits. Mag. 750X.
below - Bottom of etch pits. 1430X.

surface of the crystal was HNO_3. A pure Zn single crystal with its basal plane was etched with 9.5N HNO_3 for only 5 sec., so the etch pits were not very deep. The surface of the crystal was so shiny that it appeared electropolished. Fig. 19 (above) shows the top of the etch pits, and Fig. 19 (below) shows the bottoms of the etch pits which were very smooth.

b. Prismatic planes. Both first and second order planes of the crystal were used for the etching experiments. A (1010) plane of the single Zn crystal (Fig. 20) was etched with 6N HCl for 85 sec. According to Fig. 20, horizontal lines parallel to the basal plane (0001) were obtained. The zigzag lines under various angles to the horizontal lines represent zinc disintegrated by the etching process, in fact the black and zigzag lines were higher than the white parts of the crystal surface. The same specimen was etched with dilute HCl (2N) for 5 min., deep etch pits appeared, which were elongated along the parallel striations. In other words, the etching process penetrated into the depth of the crystal in between the basal planes. The etch pits were rare and large (Fig. 21). The same specimen etched with 12N HCl for 10 sec. developed deep, large etch pits of a form as shown in Fig. 22. The same crystal was etched with 8N HNO_3 for 10 sec., the etching pattern was almost similar to what was obtained with HCl, but no ridged zig-zag lines were observed. More dark material accumulated along the horizontal lines which were higher than the white

Figure 20.
Zn (99.999+%), single crystal, prismatic plane 1st. order, etched in 6N HCl for 85 sec. Magnification 750X.

Figure 21.
Zn (99.999+%), single crystal, prismatic plane 1st. order, etched in 2N HCl for 5 min. Magnification 1430X.

Figure 22.
Zn (99.999 %), single crystal, prismatic plane 1st. order, etched in 12N HCl for 10 sec. Magnification 1430X.

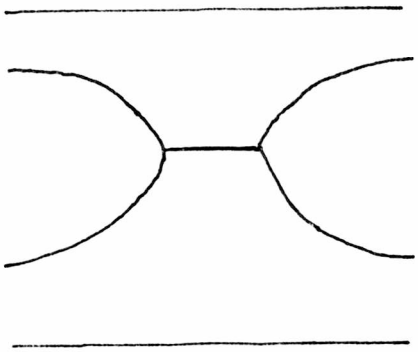

Sketch of etch pit as shown in Fig. 22.

Figure 23.
Zn (99.999+%), single crystal, prismatic plane 1st. order, etched in 8N HNO_3 for 10 sec. Magnification 145X.

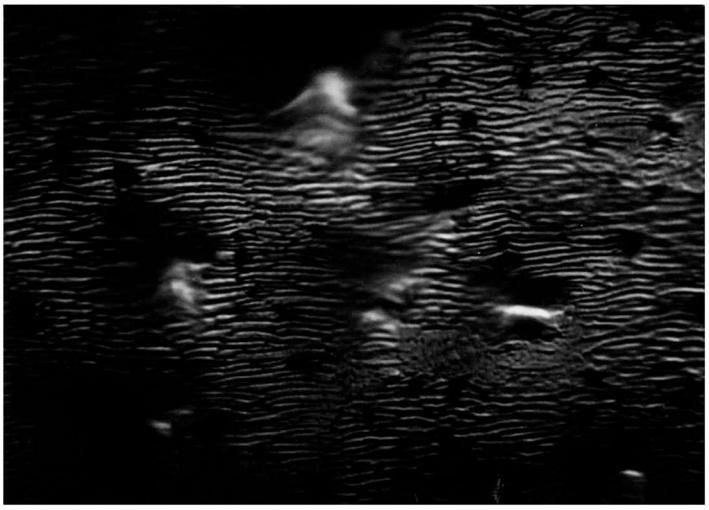

Figure 24.
Zn (99.999+%), single crystal, prismatic plane 2nd. order, etched in 9N HCl for 25 sec. Magnification 1430X.

part of the crystal surface (Fig. 23).

A specimen with a cut parallel to the $(11\bar{2}0)$ plane was etched with 9N HCl for 25 sec. Very irregular etch pits with curved background lines were obtained (Fig. 24). Black points were present on the surface of the specimen. The direction of the curved lines was in general parallel to the basal planes. A pure Zn single crystal with the same (1120) plane was etched with 8N HNO_3 for 5 sec. Pyramidal etch pits making nearly a right angle with the surface of the crystal were observed. The background of this etching pattern was not smooth (Fig. 25).

c. Pyramidal plane. The fourth crystallographic plane used for etching was the (0111) pyramidal plane. The purest Zn single crystal with this pyramidal plane was etched with 9N HCl for 2 min. After prolonged etching, the black particles were so numerous as to constitute a black network on the surface of the crystal. Some black particles were scattered within the network which was higher than the white horizontal striations. The horizontal lines were parallel to the basal plane (Fig. 26).

d. Zn-Au alloys - the basal plane. Hexagonal etch pits were observed on the (0001) surface of alloy No. 1 (0.01% Au) when it was etched with 9.5N HNO_3 for 3 sec. (Fig. 27). When Alloy No. 2 (0.02% Au) was slightly etched with dilute (2N) HCl for 20 sec., rounded etch pits were formed on the surface of the crystal. Figs. 28 and 29 were obtained on the same surface. These were typical

Figure 25.
Zn (99.99%), single crystal, prismatic plane 2nd. order, etched in 8N HNO_3 for 5 sec. Magnification 750X.

Figure 26.
Zn (99.999+%), single crystal, pyramidal plane, etched in 9N HCl for 2 min. Magnification 750X.

etching patterns using dilute HCl.

When the concentration of HCl was increased to 6N, three Zn-Au alloys showed three different etch figures. Hexagonal etch pits with corroded bottoms appeared on the basal surface of alloy No. 1 (0.01% Au). The depth of the etch pits was about 4.5 microns. (Fig. 30). Black "branches" were produced on the surface of alloy No. 2 (0.02% Au) (Fig. 31). The branches were the ridges which were higher than the white background. The particles from disintegration remained on the surface. A thin film was formed on the surface of alloy No. 3 (0.04% Au) and a crack through the thin film can be seen in Fig. 32.

e. <u>The prismatic plane.</u> The (1010) surface of alloy No. 3 (0.04% Au) was etched with 2N HCl for 2 min. Dark material accumulated on the entire surface. The white horizontal lines were parallel to the basal plane (Fig. 33).

The black particles were removed from the strongly etched surface of alloy No. 2 (0.02% Au) by a piece of scotch tape, and were observed under the reflecting light of the microscope. If the particles were observed against the shiny background, they appeared brownish dark; if removed from the shiny background, the largest part of the particles appeared white. If observed under transmitted light, they were completely dark (Fig. 34). Deposits on alloys 2 and 3, obtained by dissolution in 1N HCl until the entire surface of the alloy was covered with the black material, were removed, washed and dried for x-ray examination.

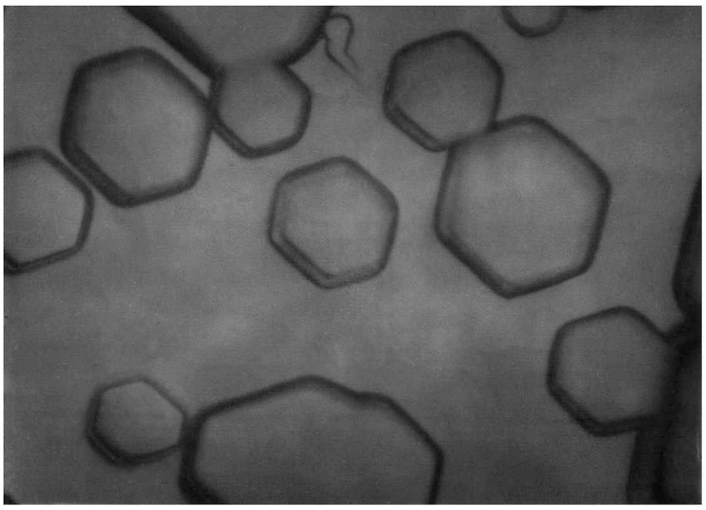

Figure 27.

Zn-Au alloy, 0.01% Au, single crystal, basal plane, etched in 9.5N HNO_3 for 3 sec. Magnification 750X.

Figure 28.
Zn-Au alloy, 0.02% Au, single crystal, basal plane, etched in 2N HCl for 20 sec. Magnification 750X.

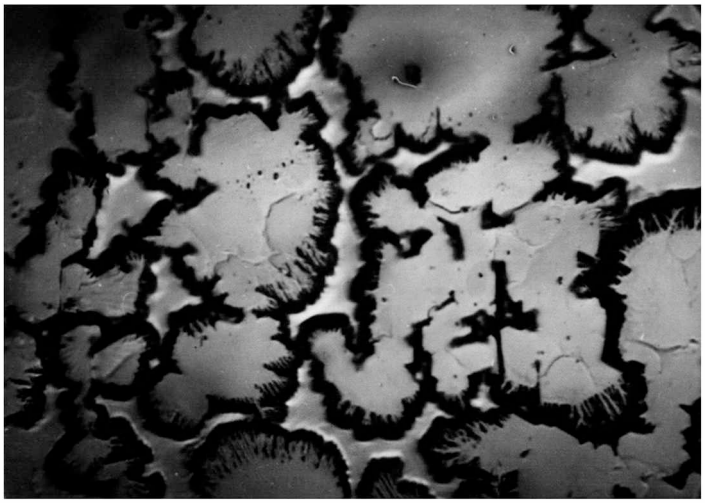

Figure 29.
Zn-Au alloy, 0.02% Au, single crystal, basal plane, etched in 2N HCl for 20 sec. Magnification 750X.

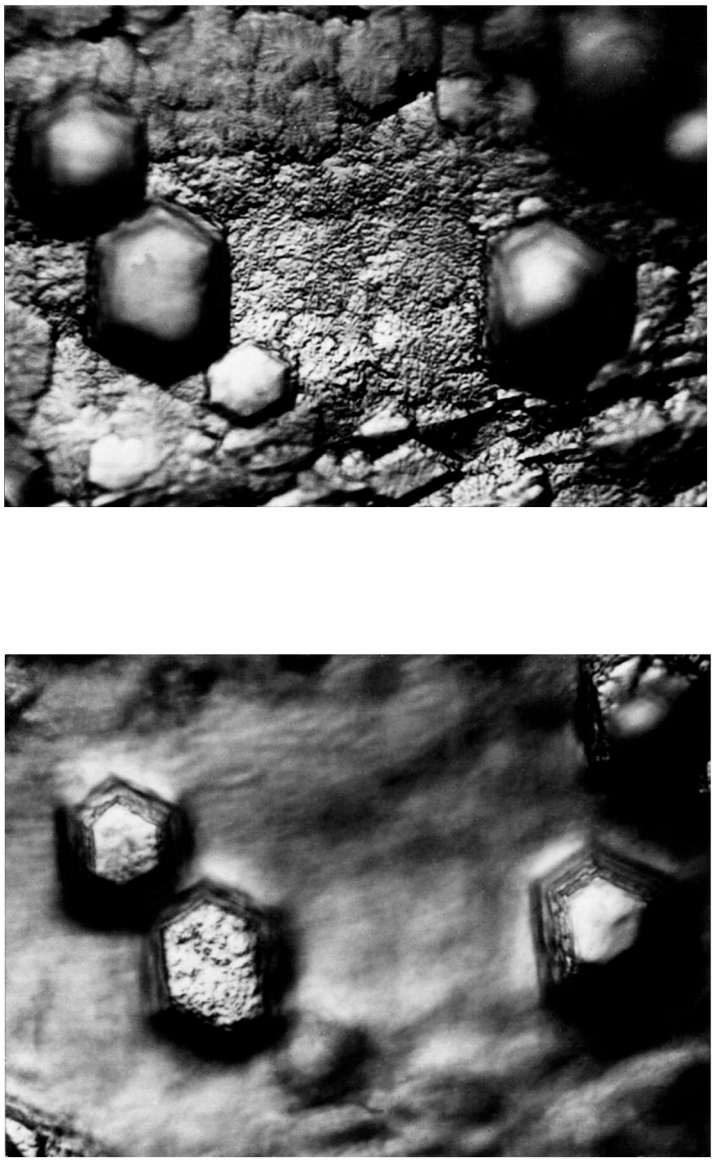

Figure 30.
Zn-Au alloy, 0.01% Au, single crystal, basal plane, etched in 6N HCl for 5 sec. Magnification 1430X.
above - Etch pits on basal plane.
below - Bottom of etch pits.

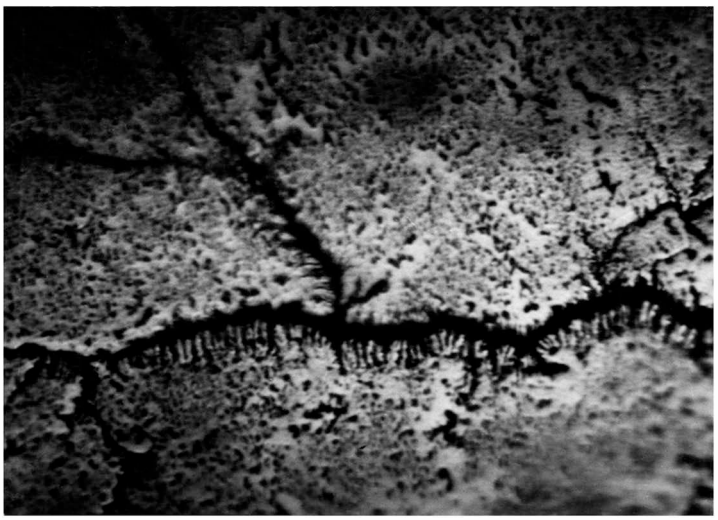

Figure 31.
Zn-Au alloy, 0.02% Au, single crystal, basal plane, etched in 6N HCl for 25 sec. Magnification 1430X.

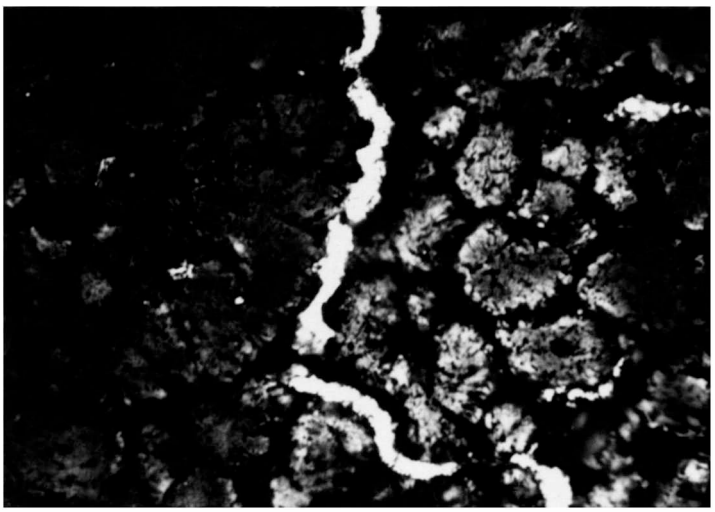

Figure 32.
Zn-Au alloy, 0.04% Au, single crystal, basal plane, etched in 6N HCl for 20 sec. Magnification 750X.

Figure 33.
Zn-Au alloy, 0.04% Au, single crystal, prismatic plane 1st. order, etched in 2N HCl for 2 min. Magnification 750X.

The x-ray pattern obtained with Cu and Co radiation were compared with those of purest zinc, and pure zinc and gold; they indicated no presence of pure zinc in the deposits. The lines on the pattern were weak and broad. Comparing the patterns with pure gold, only some very weak gold lines could be seen on the pattern of the deposits. There were other lines which could not be identified and which in all probability belonged to a zinc and gold alloy. Therefore, the deposit contained initially considerable zinc which probably was dissolved in conduct with gold.

f. Zn-Al alloys - the basal plane. An uneven (0001) surface of a crystal containing small amount of Al as low as 0.005% was revealed by etching with 6N HCl for 15 sec. According to Fig. 35, there were several "steps" on the surface of the crystal. The displacement of the fringes was about one half of the fringe separation. According to the Reichert manual of 1963, "While on a plane surface the interference fringes are straight lines parallel and equidistant to each other, any departure from true flatness produces a displacement of the fringes. This displacement is a measure for the depth of this irregularity, a deviation by one nth part of a fringe spacing corresponding to a depth $t = \lambda/2n$." In this equation λ is the wavelength of the light (illumination from the standard Low-voltage Lamp "Lux FN" with the yellow Interference Filter No. 8268, $\lambda = 0.589$ microns). Now if $n=2$ and $\lambda = 0.589$ microns, $t = 0.589/2x2 = 0.00015$ mm. The spot with the step of

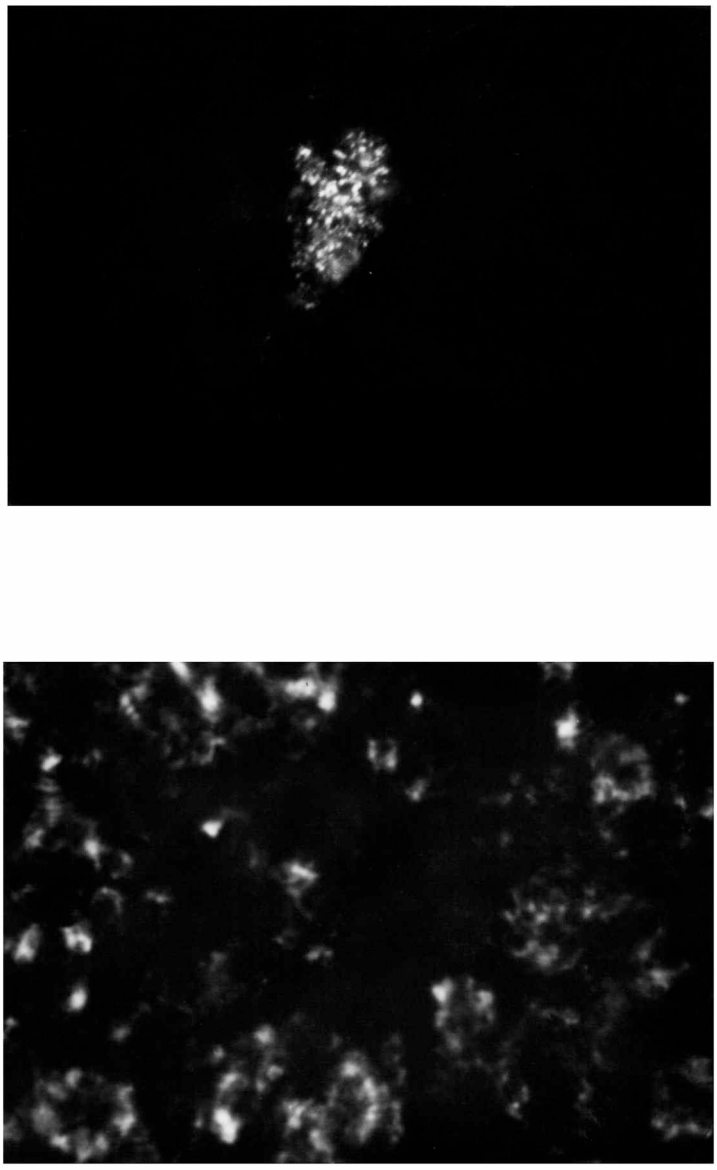

Figure 34.
Black particles removed from basal plane of Zn-Au alloy (0.02% Au) etched in 12N HCl for 5 sec. Mag. 1430X.
above - under reflected light.
below - under transmitted light.

0.00015 mm is shown at the top of Fig. 35. The other steps were nearly the same. When the same crystal was etched with very strong (12N) HCl for 10 sec., the surface became smooth. Fig. 36 shows equidistant fringes in the form of nearly perfect circles around the point of contact with the interference objective. This indicates that the bottom of the etch pit was slightly curved. As the interference tester contacted several other points around the etch pit, some irregular fringes appeared. No displacement of parts of the fringes were observed.

Fig. 37 is a representative photomicrograph of a Zn-Al alloy single crystal containing 0.025% Al. Very small etch pits were arranged in rows and the pits were shallow. If examined through an interference objective, the surface was smooth. Because of the numerous etch pits, the fringes were not perfect. The displacement of the fringes due to the etch pits was about one half of the fringe spacing. According to the equation, $t = \lambda/2n$, $\lambda = 0.589$ microns, $n = 2$, $t = 0.589/2x2 = 0.00015$ mm. It means that the depth of the etch pits was 0.00015 mm. The same crystal (Fig. 38) was strongly etched with 12N HCl for 5 sec. The surface became uneven, a very irregular fringe pattern appeared. The displacement of the fringes was not the same. (Fig. 39). There were two big etch pits as shown in this Figure, the fringe bands were nearly straight lines with equal spacing, indicating that the bottom of the etch pits was very even.

Figure 35.

Zn-Al alloy, 0.005% Al, single crystal, basal plane, etched in 6N HCl for 15 sec. Interference pattern. Mag. 165X.

Figure 36.

Zn-Al alloy, 0.005% Al, single crystal, basal plane, etched in 12N HCl for 10 sec. Interference pattern. Mag. 165X.

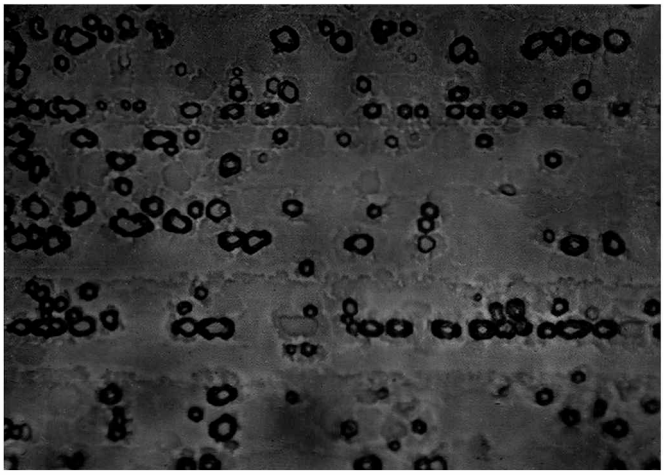

Figure 37.

Zn-Al alloy, 0.025% Al, single crystal, basal plane, etched in 2N HCl for 20 sec. Magnification 750X.

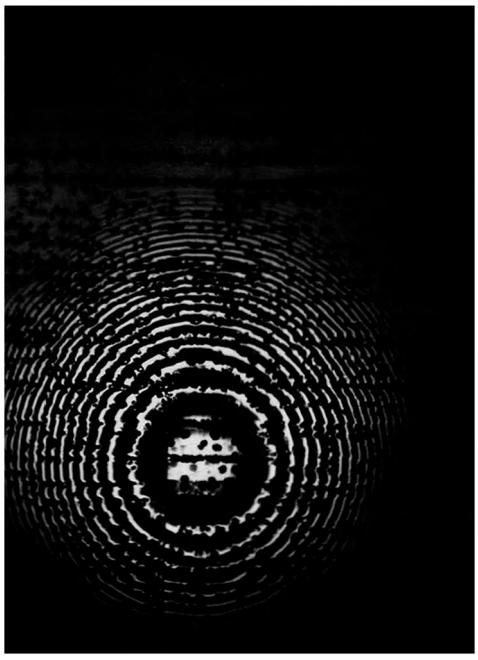

Figure 38.

Zn-Al alloy, 0.025% Al, single crystal, basal plane, etched in 2N HCl for 20 sec. Interference pattern. Mag. 165X.

Fig. 40 shows a deform twin which was not attacked as much as the surface of the crystal itself (containing 0.05% Al). The pattern was produced with dilute (2N) HCl in 20 sec. The surface of this crystal was covered with many small etch pits. The fringes showed very small deflection, about 1/20 of the fringe spacing, so, n=20, t=0.589/2x20 = 0.000015 mm. The deformation twins appeared to be higher than the other parts of the crystal.

g. The prismatic plane. The same crystal (Fig. 40) with an exposed (1010) surface was strongly etched with concentrated HCl. Rectangular etch pits were formed and particles in the center of each of the etch pits were also observed (Fig. 41).

From these figures, it was declared that Zn-Al alloys with more aluminum content are etched more easily than the alloy containing less aluminum.

h. Zn-Mg alloys - the basal plane. Although the (0001) surface of a Zn-Mg alloy (0.005% Mg) seemed to be quite even the interference objective showed a discontinuity: a fringe "step" was observed on the surface. The displacement of the fringes was of the order of one fifth of the spacing, i.e., n=5, λ=0.589 microns, t = 0.589/2x5 = 0.000060 mm. (Fig. 42). After the sample was etched with 2N HCl for 20 sec., very small etch pits were produced. The deformation twins intersected with the horizontal lines at 30 degrees (Fig. 43). When the same crystal was etched with concentrated HCl for 10 and 20 sec. consecutively, the black

Figure 39.

Zn-Al alloy, 0.025% Al, single crystal, basal plane, etched in 12N HCl for 5 sec. Interference pattern. Magnification 165X.

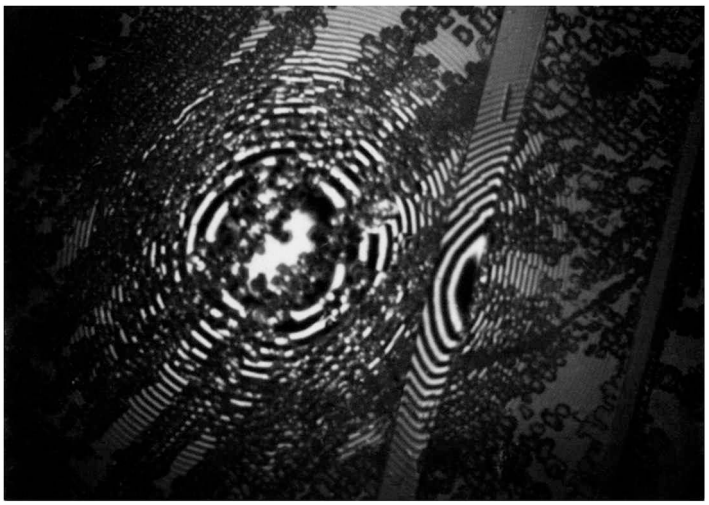

Figure 40.

Zn-Al alloy, 0.05% Al, single crystal, basal plane, etched in 2N HCl for 20 sec. Interference pattern. Mag. 165X.

Figure 41.

Zn-Al alloy, 0.05% Al, single crystal, prismatic plane 1st. order, etched in 12N HCl for 5 sec. Magnification 750X.

branches were obtained. The white part of the surface was etched down to a position which was lower than the black branches. (Fig. 44). At the etching time of 20 sec., the black particles were spread all over the surface (Fig. 45).

Etching the second crystal of Zn-Mg alloy (0.01% Mg) with 2N, 6N, and 12N HCl respectively, formed very shallow etch pits, and even the deformation twin was not attacked (Fig. 46). The black branches were produced on the surface, when the same crystal was etched in the strong acid (6N HCl) for 5 sec. The black branches were the ridges and were higher than the white background (Fig. 47). When the etching time was prolonged to 30 sec., even the deformation twin was severely attacked and the etch pits were enlarged. (Fig. 48). When the same crystal was etched with concentrated HCl for 5 sec., its surface became very shiny. It was more mirror-like than that of pure zinc and of Zn-Au alloys. Big etch pits were formed, two of them are shown as in Fig. 49. The black particles disintegrated from the crystal were also observed. The surface of the crystal became very dark and the white portions appeared in form of lines. (Fig. 49).

The third crystal used for the etching experiments was a Zn-Mg alloy with 0.025% Mg. It was etched with dilute (2N) HCl for 1 min. Many etch pits were produced on the surface of the crystal. Fig. 50 shows several deformation twins attacked by the acid. The deformation twins inter-

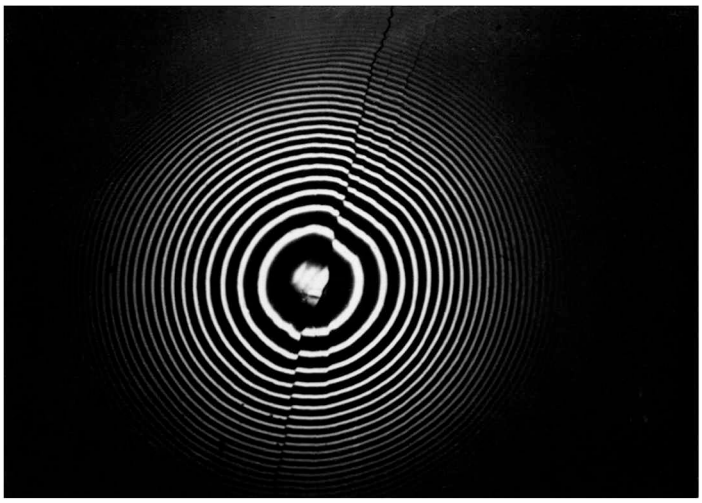

Figure 42.
Zn-Mg alloy, 0.005% Mg, single crystal, basal plane. Interference pattern of unetched cleavage surface. "step" on the surface. Magnification 165X.

Figure 43.
Zn-Mg alloy, 0.005% Mg, single crystal, basal plane, etched in 2N HCl for 20 sec. Magnification 145X.

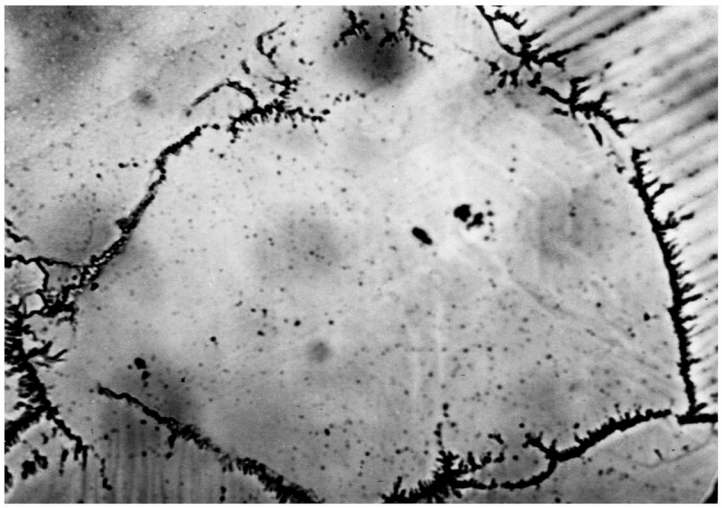

Figure 44.
Zn-Mg alloy, 0.005% Mg, single crystal, basal plane, etched in 12N HCl for 10 sec. Magnification 1430X.

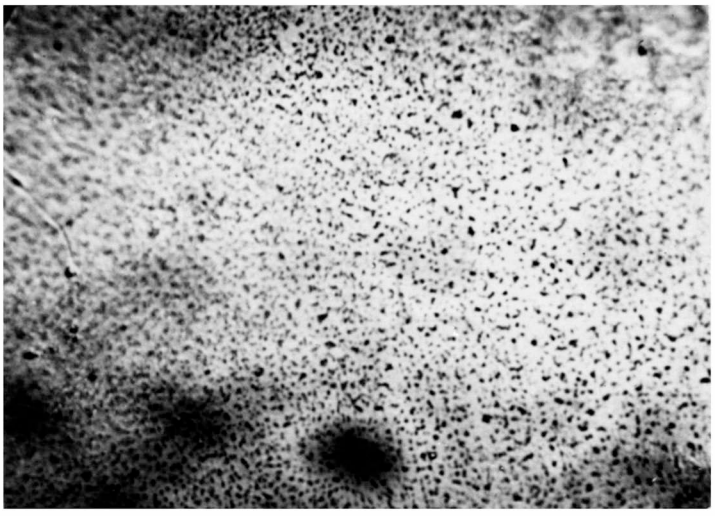

Figure 45.
Zn-Mg alloy, 0.005% Mg, single crystal, basal plane, etched in 12N HCl for 20 sec. Magnification 1430X.

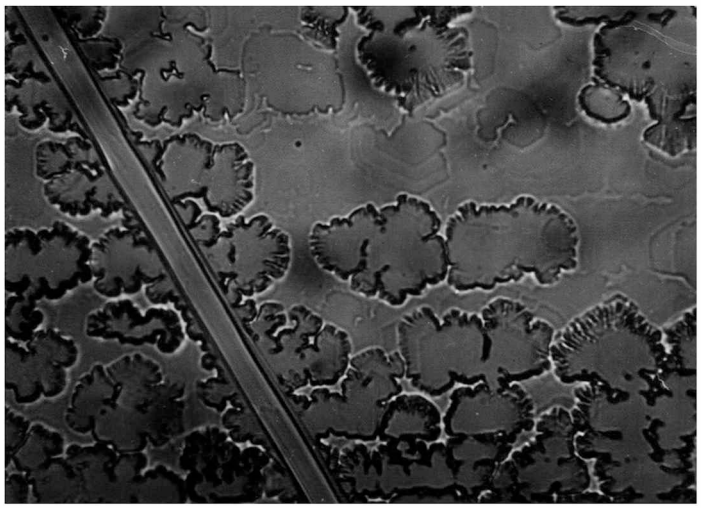

Figure 46.
Zn-Mg alloy, 0.01% Mg, single crystal, basal plane, etched in 2N HCl for 20 sec. Magnification 750X.

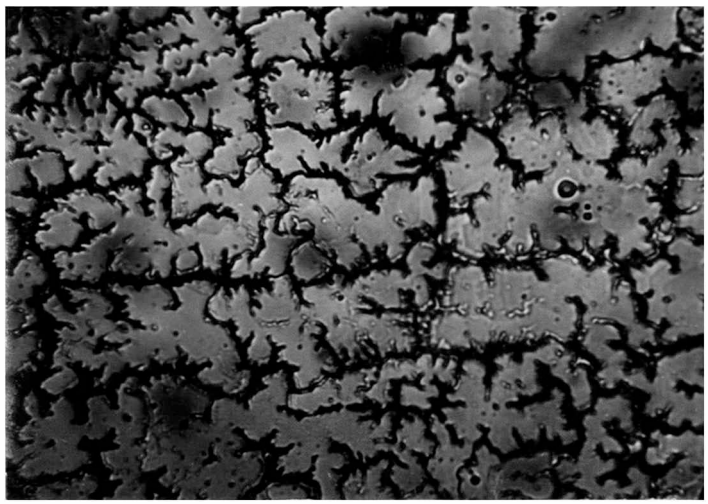

Figure 47.
Zn-Mg alloy, 0.01% Mg, single crystal, basal plane, etched in 6N HCl for 5 sec. Magnification 750X.

Figure 48.
Zn-Mg alloy, 0.01% Mg, single crystal, basal plane, etched in 6N HCl for 30 sec. Magnification 1430X.

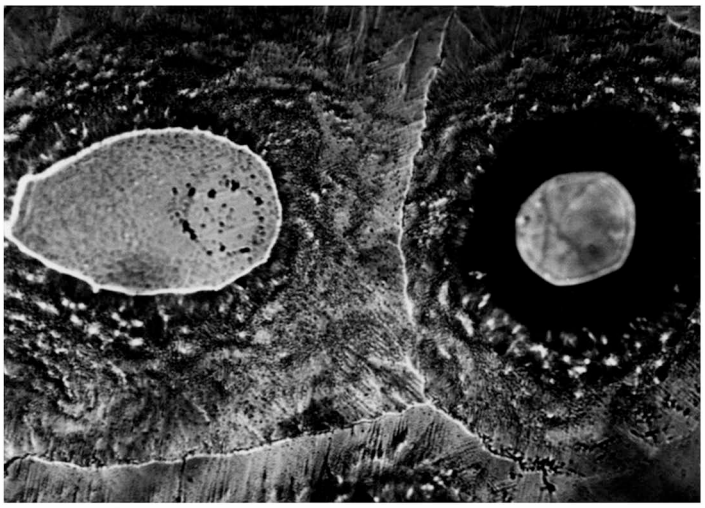

Figure 49.
Zn-Mg alloy, 0.01% Mg, single crystal, basal plane, etched in 12N HCl for 5 sec. Magnification 320X.

sected each other at 120 degrees (Fig. 50).

i. The prismatic plane. The $(10\bar{1}0)$ surface of a Zn-Mg single crystal (0.01% Mg) was etched with concentrated HCl for 5 sec. A surface with steps was developed and the particles were found scattered on the surface. The horizontal lines were parallel to the basal plane. (Fig. 51).

According to these experiments, Zn-Mg alloys are easily etched. A comparison can be made between Fig. 12 and 47, the purest Zn single crystal was etched with 9N HCl for 15 sec., and "branches" were observed on the surface. (Fig. 12). However, a Zn-Mg alloy crystal (0.01% Mg) resulted in more "branches" when it was etched with 6N HCl for only 5 sec. (Fig. 47). The etching effect was promoted by adding Mg to the pure zinc metal.

j. Anodic etching in acids. The second part of the etching experiments was anodic etching. The pure zinc single crystal was used as an anode and connected with the positive terminal of the battery. A platinum electrode was used as a cathode. The battery, the resistance box, the ammeter or milliammeter, and the two electrodes immersed into the electrolyte were connected in series. The electrolytes used were HCl, H_2SO_4, $HClO_4$, and HNO_3.

For the preliminary test a polycrystalline zinc specimen was used as an anode; it was etched in 2N HCl at 1000 ma cm^{-2} for 50 sec. Black particles appeared on the surface of the specimen (Fig. 52). The particles were partially transferred to a glass slide and were examined under high

Figure 50.
Zn-Mg alloy, 0.025% Mg, single crystal, basal plane, etched in 2N HCl for 1 min. Magnification 750X.

Figure 51.
Zn-Mg alloy, 0.01% Mg, single crystal, prismatic plane 1st. order, etched in 12N HCl for 5 sec. Magnification 1430X.

magnification with oil immersion. The particles had metallic luster and floated in the oil. The sample was entirely black in transmitted light.

After this run, the (0001) surface of a pure Zn single crystal was etched in the same electrolyte at 1000 ma.cm^{-2} for 10 sec. Hexagonal etch pits were observed. The top and the bottom of the etch pits was photographed (Fig. 53). The depth of the etch pits was about 5.5 microns. Furthermore, the $(10\bar{1}0)$ plane (prismatic) of the same crystal was etched in the same electrolyte at 1000 ma cm^{-2} for 15 sec. The crystal structure was revealed as shown in Fig. 54. The horizontal lines were parallel to the basal plane. Upon further anodic etching at higher current densities, 1-1.5 amp cm^{-2} for 75 sec., black particles accumulated on the surface of the crystal, and the horizontal lines appeared more clearly (Fig. 55). Finally, the $(11\bar{2}0)$ surface of the crystal was etched in the same electrolyte at 1000 ma.cm^{-2} for 105 sec. A multitude of black particles was observed on the surface of the crystal. The horizontal lines were curved, but were generally parallel to the basal plane (Fig. 56). In conclusion, the pyramidal plane, $(01\bar{1}L)$ of the same crystal was etched in the same electrolyte at 1000 ma.cm^{-2} for 1 min. "Grooves" with black particles were observed. The black particles shown in Fig. 57 are higher than the "grooves".

The (0001) surface of a pure Zn single crystal was etched in 2N H_2SO_4 at 625-1000 ma cm^{-2} for 40 sec. Irregular

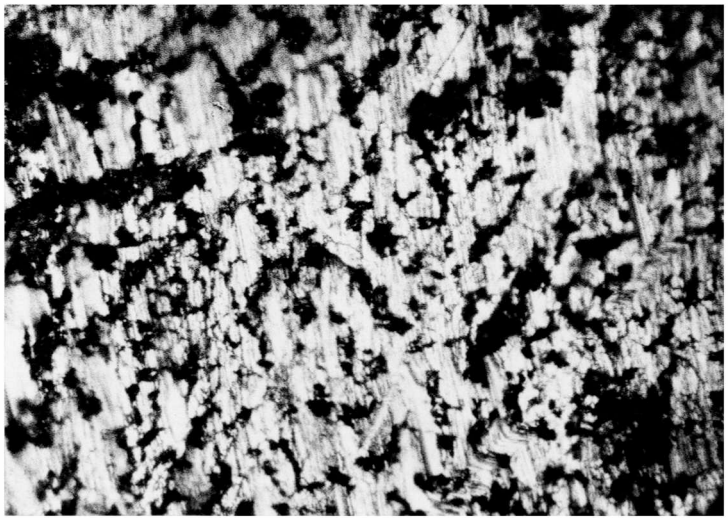

Figure 52.
Zn (99.99%), polycrystalline, etched anodically in 2N HCl for 50 sec., 1000 ma cm^{-2}. Dark deposits. Magnification 320X.

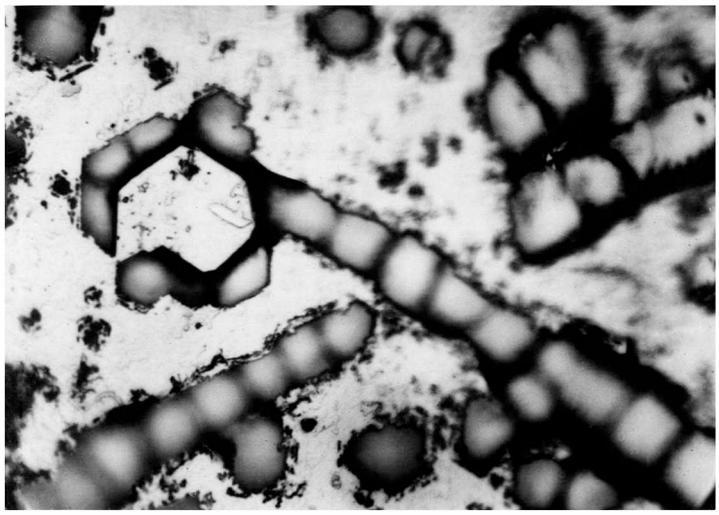

Figure 53.

Zn (99.99%), single crystal, basal plane, etched anodically in 2N HCl for 10 sec. 1000 ma cm^{-2}. Mag. 575X.
above - Upper level of the etch pits.
below - Bottom of etch pits.

Figure 54.
Zn (99.99%), single crystal, prismatic plane 1st order, etched anodically in 2N HCl for 15 sec. 1000 ma cm. Mag. 145X.

Figure 55.
Zn (99.99%), single crystal, prismatic plane 1st. order, etched anodically in 2N HCl for 75 sec. 1-1.5 amp cm^{-2}.
Black particles are present. Mag. 1430X.

etch pits were observed, but no particles were evident (Fig. 58). During electrolysis, the current could not be maintained at 1000 ma for more than 40 sec.

The (0001) surface of a pure Zn single crystal was etched with 0.5, 1, and 2N $HClO_4$ and the current density was varied from 0.5-2.5 amp cm^{-2}. The time used for electrolysis was changed from 1.5 min. to 10 sec. Fig. 59 shows only one part of the etch pits having "steps", evidently because the crystal was etched for a longer time. Fig. 60 shows nearly perfect hexagonal etch pits. On Fig. 61 very small round etch pits can be seen produced by slow etching in 2N $HClO_4$.

The (0001) surface of a pure Zn single crystal was further etched in 9.5N HNO_3 at 1000 ma cm^{-2} for 5 sec. The surface looked as if electropolished, it was very shiny and even with no etch pits on it (Fig. 62).

In conclusion it can be said that single Zn crystals partially disintegrate if subjected to anodic etching, especially at high current densities. The amount of disintegrated material may accumulate with time. Hydrochloric acid was the most effective etchant in producing various etching patterns and in disintegrating the material. The patterns on Zn single crystals formed during anodic etching changed with the use of different electrolytes.

C. <u>The Study of Anodic Disintegration of Zinc Crystals in Bromate Solutions.</u>

Neutral salt solutions had to be used for determining

Figure 56.
Zn (99.99%), single crystal, prismatic plane 2nd. order, etched anodically in 2N HCl for 105 sec. 1000 ma cm. Magnification 1430X.

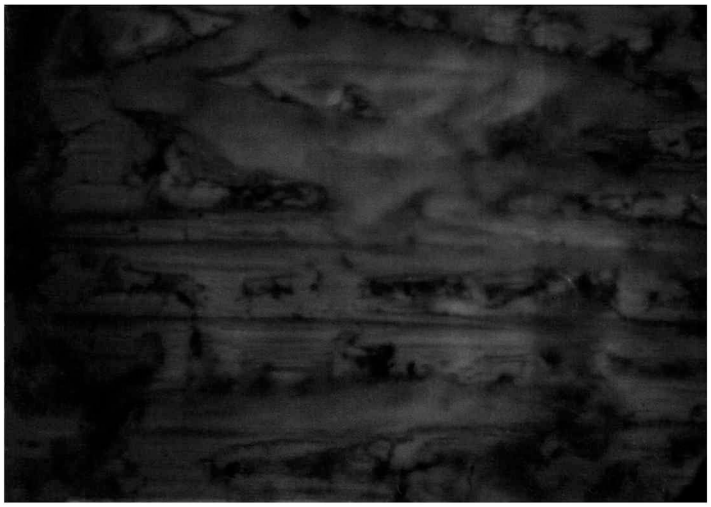

Figure 57.
Zn (99.99%), single crystal, pyramidal plane, etched anodically in 2N HCl for 1 min. 1000 ma cm^{-2}. Mag. 1430X.

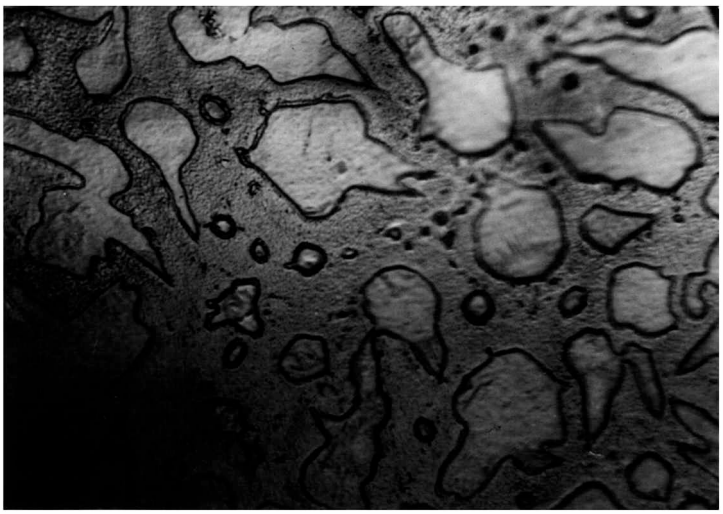

Figure 58.
Zn (99.99%), single crystal, basal plane, etched anodically in 2N H_2SO_4 for 40 sec. 625-1000 ma cm^{-2}.
Magnification 575X.

Figure 59.
Zn (99.99%), single crystal, basal plane, etched anodically in 0.5N $HClO_4$ for 1.5 min. 2-2.5 amp cm. Magnification 1430X.

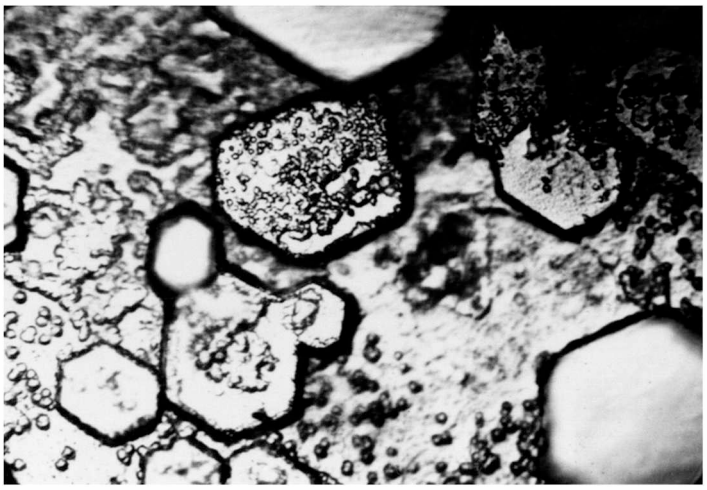

Figure 60.
Zn (99.99%), single crystal, basal plane, etched anodically in 1N $HClO_4$ for 10 sec., 1100 ma cm^{-2}. Magnification 750X.

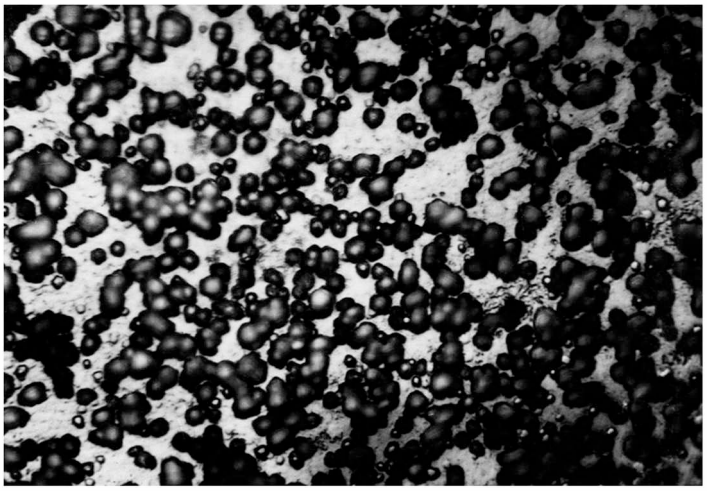

Figure 61.
Zn (99.99%), single crystal, basal plane, etched anodically in 2N $HClO_4$ for 10 sec., 500 ma cm^{-2}. Magnification 575X.

Figure 62.
Zn (99.99%), single crystal, basal plane, etched anodically in 9.5N HNO_3 for 5 sec., 1000 ma cm^{-2}. Magnification 575X.

quantitatively the degree of disintegration of zinc. The weight of zinc dissolved in 3 percent KNO_3 solution was 0.0722 grams as determined by titration with disodium EDTA, the weight of zinc that should be obtained according to Faraday's Law was 0.0671. The surface area of the anode was 1.54 cm^2; the current was kept at 0.100 amp. and the time of electrolysis was 1980 sec. at a current density of about 65 ma cm^{-2}. An apparent valence of zinc was 1.86 in agreement with the value reported in previous studies[17]. Therefore, about 0.0051 grams in excess of dissolution expected was due to the partial disintegration of zinc in nitrate solution. Were there any other salt solutions except the nitrate solutions which could cause the partial disintegration of zinc when it dissolves anodically? In answer to this question, extensive work has been done using several salts such as sodium phosphate, chromate and permanganate solutions. None of these salts showed the properties as did nitrate salts. However, chlorate solutions have been reported to produce disintegration[21]. Further experiments were made with bromate solutions. It was found that they promote the disintegration as nitrate solutions did. However the apparent valence of zinc in 3 percent $NaBrO_3$ solution was smaller than that obtained in nitrate solutions. The test run was arranged as follows:

A polycrystalline anode with a surface area of

1.54 cm^2 was dissolved in 3 percent $NaBrO_3$ solution at 0.100 amp for 1260 sec. The amount of zinc dissolved in the solution, determined by titration with disodium EDTA, was 0.06049 grams. The amount of zinc which should have dissolved in bromate solution according to Faraday's Law was 0.04268 grams. An apparent valence of 1.41 was found corresponding to a disintegration percentage of 29.4 percent.

1. Apparatus. The same arrangement was used for anodic etching of zinc single crystals. The further necessary equipment was: a micro burette of 10 ml. capacity with 0.02 ml. graduations, 2 pipettes each constructed to deliver 5 ml., a 200 ml. volumetric flask, a 100 ml. cylinder, 3 500 ml. Erlenmeyer flasks, and a 150 ml. beaker. The procedure is described in the Appendix.

2. Data and Results. The anodic dissolution of zinc in sodium bromate solutions was carried out at room temperature in a 3 percent (by weight) solution at several current densities with different zinc crystals as anodes. The data obtained in these runs are given in Tables IV-VII. The average value for the apparent valence of zinc ions in bromate solutions was 1.45$\pm$ 0.02, indicating that the zinc dissolved anodically in bromate solutions gave a much smaller apparent valence than its normal valence of plus two.

During the anodic dissolution of zinc in bromate solutions, the current decreased gradually during 5-10 minutes, and depends on the amount of passing current. At a low current such as 0.030 amp, the current could be

TABLE IV.

Apparent valence of zinc (99.99% polycrystalline) dissolving anodically in a 3 percent $NaBrO_3$ solutions

Surface Area - 1.54 cm^2

Time sec.	Current amp	Wt. of Zinc Exptl. g.	Calcd. g.	Apparent Valence	Disintegration IN %
850	0.240	0.0962	0.0691	1.44	28%
720	0.240	0.0837	0.0585	1.40	30%
743	0.240	0.0858	0.0604	1.41	29%
			Average	1.42	29%
Zinc (99.99%) single crystal, (0001) plane, surface area -0.94 cm^2					
1380	0.145	0.0965	0.0678	1.40	30%
1380	0.145	0.0964	0.0678	1.41	30%
840	0.145	0.0617	0.0413	1.37	33%
			Average	1.39	31%

TABLE V.

Apparent valence of zinc (99.99+%) dissolved anodically in 3 percent $NaBrO_3$ solution.

(0001) plane surface area - 1.65 cm^2

Time sec.	Current amp	Wt. of Zinc Exptl. g.	Calcd. g.	Apparent Valence	Disintegration in %
570	0.255	0.0691	0.0492	1.42	28.2%
3960	0.085	0.1585	0.1140	1.44	21.8%
			Average	1.43	25%
Zinc single crystal (99.999+%) (0001) plane, surface area = 0.71 cm^2					
1260	0.110	0.0652	0.0470	1.44	28%
1560	0.110	0.0781	0.0581	1.49	25.6%
1020	0.110	0.0503	0.0380	1.51	24.5%
1020	0.110	0.0523	0.0380	1.45	27.3%
			Average	1.47	26.4%
$(10\bar{1}0)$ plane surface area - 0.45 cm^2					
1800	0.070	0.0591	0.0427	1.44	27.8%
(1120) plane surface area - 0.55 cm^2					
1800	0.085	0.0703	0.0518	1.47	26.3%

TABLE VI.

Apparent valence of zinc dissolved anodically in 3 percent $NaBrO_3$ solution. Zn-Au alloy (1% Au), polycrystalline

Surface area - 1.08 cm^2

Time sec.	Current amp	Wt. of Zinc Exptl. g.	Calcd. g.	Apparent Valence	Disintegration in %
1260	0.170	0.0957	0.0725	1.52	24.2%
1200	0.170	0.0868	0.0691	1.59	20.4%
1200	0.170	0.0877	0.0691	1.57	21.2%
			Average	1.56	21.9%

Single crystal of Zn-Au alloy (0.01% Au), (0001) plane

Surface area - 1.17 cm^2

1140	0.180	0.927	0.0695	1.49	25%
1260	0.180	0.1008	0.0768	1.52	24%
980	0.180	0.0838	0.0598	1.43	28.6%
			Average	1.48	25.8%

TABLE VII.

Apparent valence of Zinc dissolved anodically in 3 percent $NaBrO_3$ solution. Single crystal of Zn-Mg alloy (0.005% Mg) (0001) plane, surface area - 0.92 cm^2

Time sec.	Current amp	Wt. of Zinc Exptl. g.	Calcd. g.	Apparent Valence	Disintegration in %
1680	0.145	0.1136	0.0825	1.45	27.4%
1560	0.145	0.1036	0.0766	1.47	26%
1440	0.145	0.0939	0.0707	1.50	24.8%
			Average	1.47	26%

Single crystal of Zn-Al alloy (0.005% Al), (0001) plane, Surface area - 1.17 cm^2

1080	0.180	0.0899	0.0659	1.46	26.8%

kept at this level for 20-30 minutes; at high current such as 0.240 amp., the current level could be maintained for only a few minutes. To maintain the desired level of the current, the resistance had to be adjusted. The zinc anode turned dark as soon as the electrolytic circuit was closed and the dark film began to spall off the anode and settle to the bottom of the beaker. Shortly after that it became white, and nearly the entire surface of the anode became white when the experiment was discontinued. The white precipitate was dissolved in dilute (2N) sulfuric acid and titrated with disodium EDTA.

3. Sample calculations. The method used for the calculation of the apparent valence in bromate solutions was the same as that used in determining the apparent valence in nitrate solutions. The data for the anodic dissolution of zinc in 3 percent sodium bromate (Table V) are used to illustrate the calculations. The apparent weight of zinc dissolved according to Faraday's Law, assuming the normal oxidation state of plus two, was calculated as follows:

$$\text{Wt. zinc (apparent)} = \frac{tI(\text{At. Wt. Zn})}{Fn}$$

where: t is the time interval of the run equal to 1020 sec.,

I the current of 0.110 amp.,

At. Wt. zinc the atomic weight of zinc equal to 65.38,

F the Faraday constant (96,500 amp. sec.) and

n the normal cationic charge of zinc (+2)

A weight of 0.0380 g. of Zn was found.

The amount of Zn obtained by titration was calculated as follows:

A 5 ml. aliquot was taken from a 200 ml. sodium bromate solution containing zinc ions.

1 ml. EDTA solution was equivalent to 0.9915 ml. of the standard zinc solution and 1 ml. of the latter contained 0.6532 g. of zinc. For titration with EDTA 2.02 ml. were used. Therefore, 2.02 x 200 / 5 = 80.8 ml. and

80.8 x 0.9915 x 0.6532 = 0.0523 g. of Zn were obtained. The apparent valence was calculated simply by means of the equation: $V = \frac{2 \times (\text{Wt. of zinc calculated})}{(\text{Wt. of zinc obtained})} =$

$$\frac{2 \times 0.0380}{0.0523} = 1.45$$

The disintegration percentage was calculated as follows:

$$\frac{(0.0523 - 0.0380)}{0.0523} \times 100 = \frac{1.43}{0.0523} = 27.3\%$$

4. <u>The study of the surface film formed on a zinc anode dissolving in sodium bromate solutions</u>. For studying the dark film on the surface, the zinc anode was taken out of the electrolyte after 20 sec. of electrolysis. It was immersed into dry acetone. The black flakes were washed, dried, and examined under a high magnification microscope using oil immersion objective. There were many small particles with metallic luster under reflected light. The particles were completely dark in transmitted light. (Fig. 63 and 64).

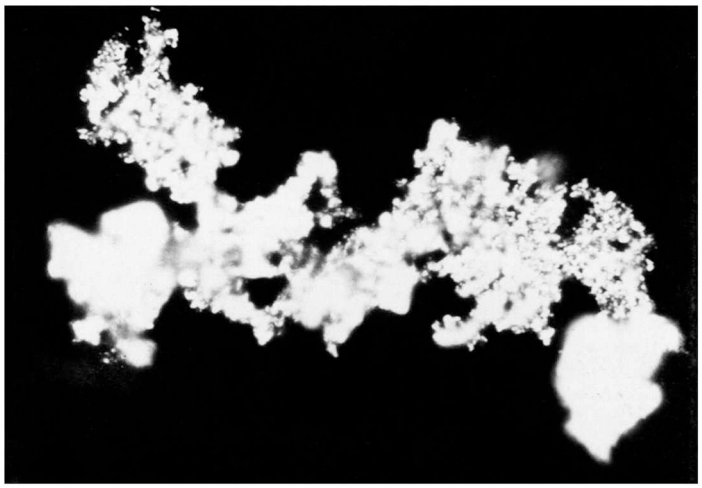

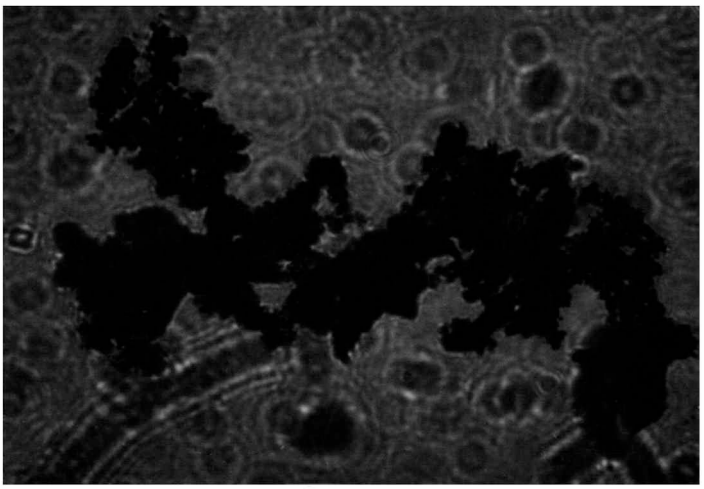

Figure 63.

Zn particles that are present in the black film obtained during anodic dissolution of zinc in 20 sec. in a 3% $NaBrO_3$ solution. Magnification 1430X.

above - Particles in reflected light.
below - Particles in transmitted light.

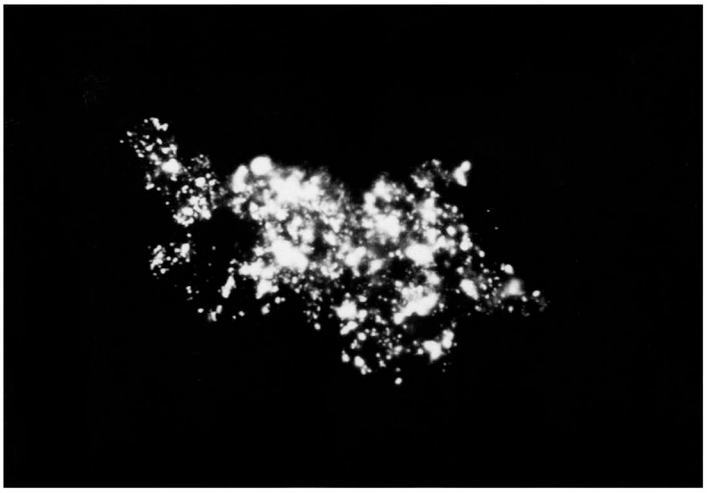

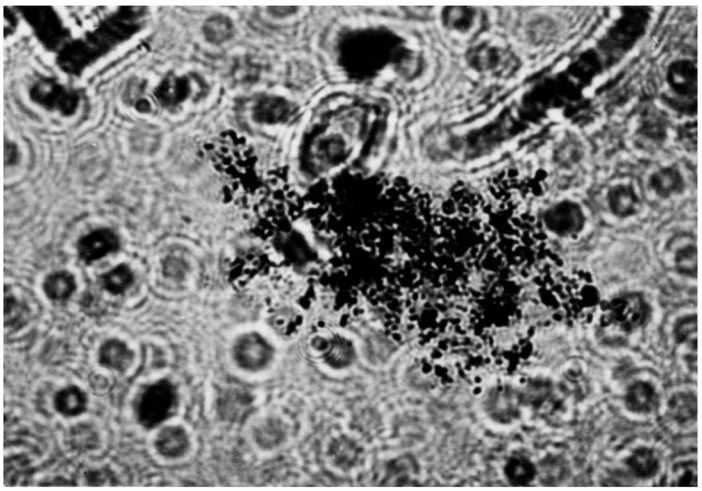

Figure 64.

Zn particles that are present in the black film obtained during anodic dissolution of zinc in 20 sec. in a 3% $NaBrO_3$ solution. Magnification 1430X.

above - Particles in reflected light.
below - Particles in transmitted light.

IV. DISCUSSION

The discussion consists of three parts: A. discussion of results, B. limitations, and C. recommendations.

A. Discussion of Results.

1. Preparation of single Zn crystals.

The preparation of single zinc crystals using the Bridgman method was satisfactory. For this research a desired orientation of the single crystals was not necessary. In most instances, the single crystals grew with the basal plane, under a certain angle with the growth axis; but some single crystals grew with the basal plane parallel to that axis. As regards the disintegration phenomena of single zinc crystals, the orientation had little if any effect.

2. Formation of etch pits.

Nearly perfect geometrical (hexagonal) etch pits were always found on the basal plane of the crystals. The etch pits observed on the three other crystallographic planes showed different characteristics.

3. Purity of single Zn crystals.

The solid solution zinc single crystals etched more easily than those of purest zinc metal. This phenomenon is consistent with the action of local currents, increasing the rate of corrosion.

4. Anodic disintegration of Zn single crystals.

Anodic dissolution of zinc in a 3 percent KNO_3 solution was performed and the apparent valence of zinc was 1.86 in agreement with previous studies[17,22].

The authors[22] suggested that the reaction of zinc in nitrate solutions was film controlled in a manner similar to that proposed for magnesium [12,23]. Anodic dissolution of zinc in 3 percent $NaBrO_3$ solution at room temperature showed an apparent valence of about 1.45 ± 0.02 which is smaller than the apparent valence of zinc in 0.2 M $KClO_3$ solution previously reported[21]. The authors[21] proposed a two-step mechanism for the anodic oxidation of zinc. The first step involves electrolytic oxidation of the metal to the unipositive ion; the second step involves the oxidation of the unipositive ion to the bipositive oxidation state by competing reactions occurring either at the electrode or in oxidizing electrolyte. In this investigation, a dark film was formed at the anode in 3 percent $NaBrO_3$ solution as soon as the electrolytic circuit was closed. The film continually spalled off the anode and formed insoluble white precipitates. Under microscopic examination, the film was observed to contain many small metallic particles. The phenomena are the same as were observed in nitrate solutions and suggest the same mechanism for the anodic disintegration of zinc in bromate solutions. According to Faraday's Law, one gram-equivalent weight of a substance is liberated by the passage of 9.65×10^4 coulombs through an electrolyte. In other words, 32.69 grams of zinc should be liberated by the passage of 9.65×10^4 coulombs through a 3 percent $NaBrO_3$ solution. The dissolution of zinc particles, which are disintegrated from zinc anode, outside the electrical circuit

thus accounts for the lower coulombic equivalent and also it causes the apparent valence of zinc dissolved in bromate solution less than its normal valence of two. The difference between the amount of zinc actually dissolved in bromate solution and the amount of zinc dissolved in the same solution according to Faraday's Law is the amount of zinc due to disintegration. The amount of zinc dissolved in bromate solution due to disintegration divided by the total amount of zinc dissolved in the same solution is the percentage of disintegration. Disintegration of anodes has been known for many years and existence of metallic particles has been confirmed in this and other studies [17,22]. The mechanism suggested below does not require the postulation of intermediate valence states. To the best knowledge of the author, no electron paramagnetic resonance studies have reported the presence of Zn^{+1} in aqueous solutions. Formation of the dark film is explained as follows:

$$2Zn^{\circ} + BrO_3^- + 2H_2O \longrightarrow 2Zn(OH)_2 + BrO^- \quad \ldots\ldots\ldots\ldots\ldots (1)$$

$$3BrO^- \longrightarrow BrO_3^- + 2Br^- \quad \ldots\ldots\ldots\ldots\ldots\ldots\ldots (2)$$

Because the very small zinc particles were very reactive and are oxidized immediately by bromate ion to form insoluble $Zn(OH)_2$ and BrO^-, the BrO^- then disproportionates into BrO_3^- and Br^- ion. The presence of the bromide ions was proved, by use of a few drops of $AgNO_3$ solution mixed with the 3 percent $NaBrO_3$ solution obtained after anodic dissolution of the Zn; which results in yellowish precipitates of AgBr, thus indi-

cating the presence of the bromide ions.

5. Anodic disintegration of zinc alloys.

When Zn-Au crystals containing 0.01% Au dissolved anodically in 3 percent $NaBrO_3$ solutions, the apparent valence was 1.48 for the (0001) plane and 1.56 for a polycrystalline Zn-Au alloy containing 1% Au. Evidently, the higher gold content in the alloy caused less disintegration of zinc.

When Zn-Al or Zn-Mg alloys dissolved anodically in the same electrolyte, apparent valences of 1.46 for Zn-Al alloy (0.005% Al) and 1.47 for Zn-Mg alloy (0.005% Mg) were obtained for the (0001) plane. Practically the results were the same and equal to that obtained with pure zinc single crystals. Thus, there was no influence of the alloying elements on the disintegration of zinc single crustals. The percentage of disintegration was about 25% in all these cases.

B. Limitations.

Limitation of solid solubility.

The limitation in the solid solubility of Mg in Zn at room temperature provided difficulties in growing single crystals, because the single crystals of Zn-Mg alloys had to cool slowly. The segregation of Mg in alloy 8 (0.01% Mg) and 9 (0.025% Mg) was observed. The growth of single crystals of Zn-Al alloys was also difficult, but single crystals of Zn-Au alloys were easily prepared because of the higher solid solubility of Au in

Zn at room temperature.

C. Recommendations.

Anodic dissolution of zinc was carried out in 3 percent $NaBrO_3$ solution at room temperature. A further study should be made of the effect of temperature and anion concentration on the apparent valence of zinc dissolving anodically. A solution of $NaBrO_3$-NaBr mixture could also be used as an electrolyte to determine the influence of halide ion on the apparent valence or percentage of disintegration.

V. SUMMARY AND CONCLUSIONS.

1. The Bridgman method was used for growing single crystals of pure zinc and its alloys. Zinc-gold, zinc-aluminum, and zinc-magnesium single crystals were grown. Each single crystal was cut along four different crystallographic directions for both chemical and anodic etching. The etch patterns were different on different crystallographic planes. The results are summarized as follows:

On (0001) plane .....geometrical (hexagonal) etch pits were produced

On $(10\bar{1}0)$ plane.....horizontal lines with elongated etch pits appeared

On $(11\bar{2}0)$ plane.....curved lines with irregular etch pits were formed and

On $(01\bar{1}L)$ plane.....grooves with very irregular etch pits appeared

2. The etchants were HCl, $HClO_4$, H_2SO_4 and HNO_3 in various concentrations. HCl was the main etchant for all the etching experiments. The etched surfaces were examined microscopically and with the interference tester.

3. Black particles appeared on the surface of the crystal or in the bottom of the etch pits due to strong etching. The maximum depth of the etch pits produced by strong etching was about 10 microns. The nature of the black particles was examined under reflected and transmitted light. The tiny black particles with metallic luster were opaque to light.

4. The anodic disintegration of zinc in 3 percent $NaBrO_3$ solution was studied. The apparent valence of zinc was

about 1.45± 0.02 corresponding to about 25% of disintegration. In other words, the amount of zinc dissolved in bromate solutions was 25 percent larger than expected from Faraday's Law. The dark film containing many small metallic particles was studied under high magnification with an oil immersion objective. The metallic regions of the film were completely dark in transmitted light. Alloying elements such as gold led to less disintegration of the crystal. As for aluminum and magnesium, they promoted the corrosion process because of their greater activity. The effect of the addition of Al or Mg to pure zinc metal for the promotion of disintegration of zinc single crystals was not distinguishable. The results obtained with polycrystalline zinc and with zinc single crystals using different crystallographic planes were nearly the same. It is concluded that the disintegration mechanism is not dependent on the crystal structure or the orientation of the crystallographic planes exposed to the electrolyte.

VI. BIBLIOGRAPHY

1. Bridgman, P. W. (1925) Certain Physical Properties of Single Crystals of Tungsten, Antimony, Bismuth, Tellurium, Cadmium, Zinc and Tin. Proceedings, American Academy of Arts and Sciences. 60, p. 305.

2. Jillson, D. C. (1950) Production and Examination of Zinc Single Crystals. Trans. AIME. 188, p. 1005.

3. Steinberg, M. A. (1951) Producing Single Crystals of Metal. Journal of Metals. May 1951, p. 387.

4. Maddin, R. and Asher, W. R. (1950) Apparatus for Cutting Metals Strain-Free. Rev. Sci. Instru. 21, p. 881.

5. Yamamoto, M. and Watanabe, J. (1956) A study on the Strain-Free Cutting of Metal Single Crystals. Sci. Rep. Tohoku University. 8, p.230.

6. Reitsma, L. J., Jr. (1959) A study of the Recrystallization and The Mechanical Properties of Indium. T. 1217 MSM, p. 100.

7. Bassi, G. and Hugo, J. P. (1959) Etch Pits in Zinc J. of Inst. of Metals. 87, p. 376.

8. Bicelli, L. P. and Rivolta B. (1961) Influence of Crystal Orientation on the Etching Process of Metallic Single Crystals. Metallurgia Italiana. 53, July 1961, p. 363.

9. Gilman, J. J. (1956) Etch Pits and Dislocation in Zinc Monocrystals. J. of Metals. Aug. 1956, p. 998.

10. George, J. (1959) Dislocation Etch Pits in Zinc Crystals. Phil. Magazine. 4, p. 1142.

11. Evans, U. R. (1960) "Corrosion and Oxidation of Metals", p. 883, Edward Arnold, London.

12. Hoey, G. R. and Cohen, M. (1958) Corrosion of Anodically and Cathodically Polarized Magnesium in Aqueous Media. Electrochem. Soc. J. 105, NO. 5, p. 245.

13. Marsh, G. A. and Schaschl, E. (1960) The Difference Effect and the Chunk Effect. J. Electrochem. Soc. 1960. p. 960.

14. Straumanis, M. E. and Mathis, D. L. (1962) The Dissolution Reaction and Attack of Beryllium by HF, HCl, and H_2SO_4. J. Electrochem. Soc. 109, No. 5, p. 435.

15. Straumanis, M. E. and Mathis, D. L. (1962) The Disintegration of Beryllium During its Dissolution in Hydrochloric Acid. J. Less-Common Metals, 4 (1962) p. 213.

16. Straumanis, M. E. and Bhatia, B. K. (1963) Disintegration of Magnesium While Dissolving Anodically in Neutral and Acidic Solutions. J. Electrochem. Soc. 110, NO. 5, p. 357.

17. James, W. J. and Stoner, G. E. (1963) Valence Exhibited by Zinc Amalgam Anodically Dissolving in Nitrate Solutions J. Amer. Chem. Soc. 85, NO. 9, p. 1354.

18. Westgren, A. and Phragmen, G. (1925) X-Ray Analysis of Copper-Zinc, Silver-Zinc, and Gold-Zinc Alloys. Phil. Magazine. 50, p. 316.

19. Hansen, M. (1958) "Constitution of Binary Alloys." McGraw-Hill Book Co., Inc. p. 150.

20. Anderson, E. A. and Rodda, J. L. (1939) "Metals Handbook" 1939 ed. pp. 1750-1751. ASM Cleveland, Ohio

21. Sorensen, D. T., Davidson, A. W. and Kleinberg, J. (1960) The Anodic Oxidation of Zinc and Cadmium in Aqueous Solution. J. Inorg. Nucl. Chem. 13, p. 64.

22. James, W. J., Stoner, G. E. and Straumanis, M. E. (1963) Anodic Disintegration of Zinc Undergoing Electrolysis in Nitrate Solutions. Technical Report No. 4. Depts. of Chem. Engr. and Chem. and of Met. Engr., MSM, Rolla, Missouri.

23. James, W. J., Straumanis, M. E., Bhatia, B. K. and Johnson, J. W. (1963) The Difference Effect on Magnesium Dissolving in Acids J. Electrochem. Soc. 110, p. 1117.

VII. Appendix

1. Preparation of standard zinc solution.

0.3266 g. of analytical grade zinc metal pellets were weighed and dissolved in strong HCl keeping the excess of acid as small as possible. After the zinc was dissolved, the solution was transferred quantitatively to a 500 ml. volumetric flask, and diluted to the mark with distilled water.

2. Preparation of disodium EDTA.

1.8612 g. of disodium EDTA transferred to 500 ml. volumetric flask dissolved in distilled water contained in a polyethylene bottle for use, and filled up to the mark with the same water.

3. Preparation of buffer solution of pH 10.

70 grams of NH_4Cl were dissolved in 570 ml. of ammonia (concentrated) and diluted with distilled water to 1 liter, and transferred to a polyethylene container.

4. Standardization of disodium EDTA.

5 ml. of standard zinc solution were taken by means of a pipette, diluted to 200 ml. with distilled water and heated to about 80°C. 10 ml. of pH 10 buffer solution were added along with one drop of Erichrome Black-T indicator solution. The solution was titrated with disodium EDTA using a micro burette until the solution turned blue. From the ml. of the EDTA solution the amount of Zn in solution was calculated.

VIII. VITA

Yun Wang was born February 10, 1919 in Shasi, Hupei, China. For his primary education he was educated at home, for his secondary education he was graduated from Hupei provincial Chiangling Middle School. In July, 1944 he received a Bachelor of Science degree from National Yunnan University at Kunming, Yunnan, China.

During World War II, he served in the Foreign Affairs Bureau of National Military Council as an Interpreting Officer, and associated with the U. S. Army in India and in China.

In March, 1947, he left Kunming for Shanghai where he worked for National Resources Commission as an Assistant Engineer. In December, 1948, he was transferred to Taiwan Steel Works at Kaohsiung, Taiwan and served as Materials Section Leader for ten years. In October, 1958, he was transferred to Taiwan Machinery Mfg. Co. in the same city, and he was assigned to be the Chief of the Production Control Section.

In July, 1948, he was married to Ya-Hsiu Kuo of Peiping in Shanghai. He has a daughter, Tien-Ming, who is attending the Junior Middle School at Kaohsiung, Taiwan.

Since February, 1963 he has been appointed by the Missouri School of Mines and Metallurgy at Rolla, Missouri as a Research Assistant in the Department of Metallurgical Engineering.